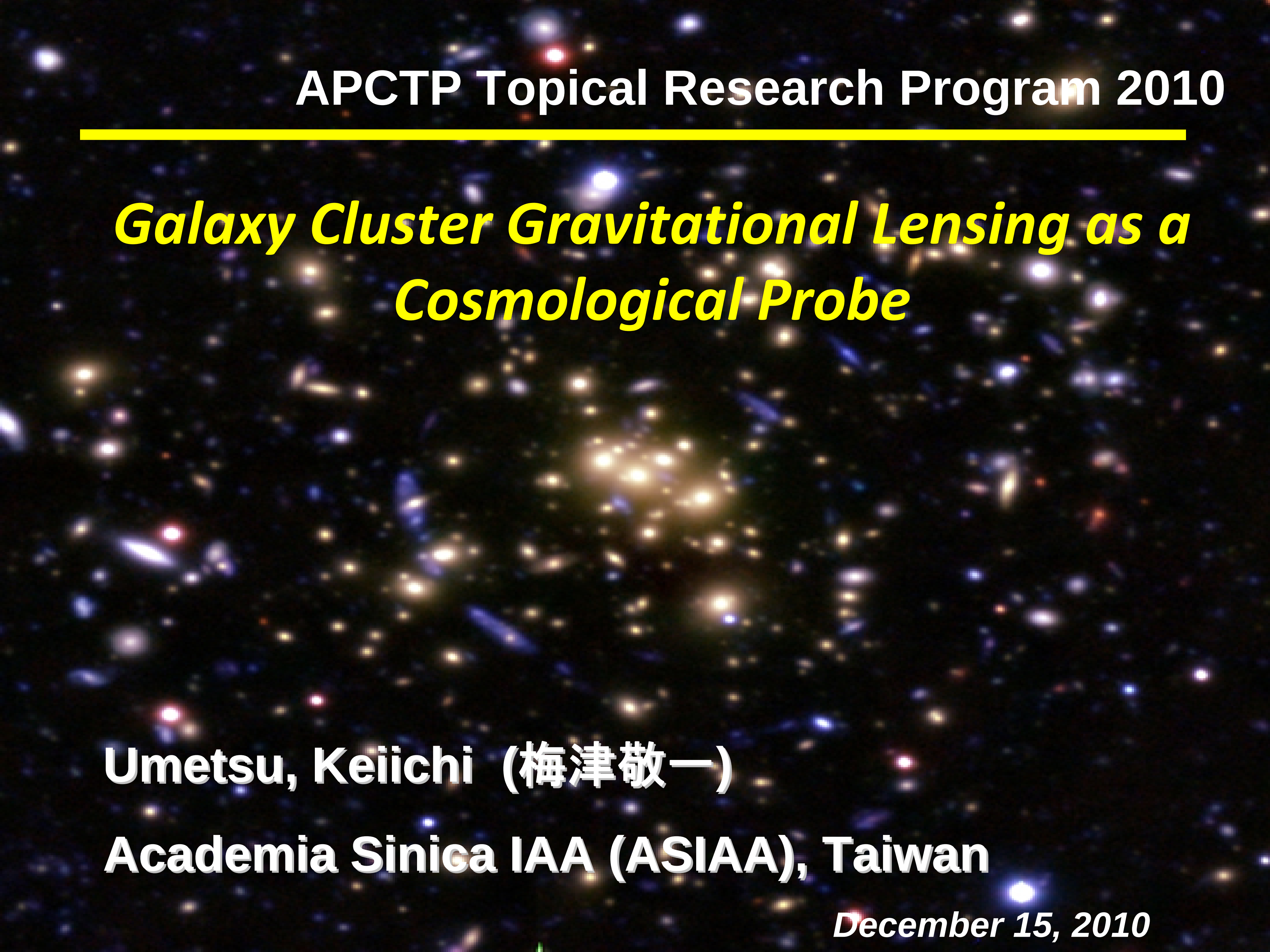

APCTP Topical Research Program 2010

Galaxy Cluster Gravitational Lensing as a Cosmological Probe

Umetsu, Keiichi (梅津敬一)

Academia Sinica IAA (ASIAA), Taiwan

December 15, 2010

Outline of My Talk

1. **Motivation and Importance of Study**
   - Galaxy Clusters as Cosmological Probes
2. **Method: Cluster Gravitational Lensing**
   - Gravitational Lensing by Galaxy Clusters in Weak and Strong Regimes
3. **Highlights**
   - Current Lensing Constraints on DM Halo Mass Profile Shapes
4. **Future Work: The Largest Space-Telescope Cluster Survey, "*CLASH*"**
   - 524-orbit Hubble Multi-Cycle Treasury (MCT) program, "Cluster Lensing And Supernova survey with Hubble" (PI: Marc Postman, STScI)
5. **Summary**

Lensing Collaborators

Tom Broadhurst (Tel Aviv U., Israel → Bilbao, Spain)
Elinor Medezinski (Tel Aviv U., Israel → STScI)
Adi Zitrin (Tel Aviv U., Israel)
Doron Lemze (Tel Aviv U., Israel → STScI)
Yoel Rephaeli (Tel Aviv U., Israel)
Nobuhiro Okabe (ASIAA, Taiwan)
Sandor Molnar (ASIAA, Taiwan)
Bau-Ching Hsieh (ASIAA, Taiwan)
Masahiro Takada (IPMU, Japan)
Masamune Oguri (NAOJ, Japan)
Toshifumi Futamase (Tohoku U., Japan)
Graham P. Smith (Birmingham U., UK)

1. Motivation and Importance:

“Galaxy Clusters as Cosmological Probes”

Concordance Structure Formation Scenario

Current paradigm of structure formation: Lambda Cold Dark Matter (LCDM)

- **Background geometry and Initial conditions**, successfully constrained by linear theory & large-scale astrophysical observations:
  - CMB, large-scale clustering of galaxies (BAO), and SNIa distance measurements
- >70% of the *"present-day"* energy density is in the form of **Dark Energy**, leading to an accelerated cosmic expansion → suppressing the structure growth in later epochs
- ~85% of our *"material universe"* is composed of unknown **DM** – the majority of which being non-relativistic, effectively collisionless (cf. the Bullet cluster)
- Study **nonlinear** cosmic structure formation due to the **gravitational instability** using N-body simulations + perturbation theory ($0 < z < z_{dec} \sim 1100$)

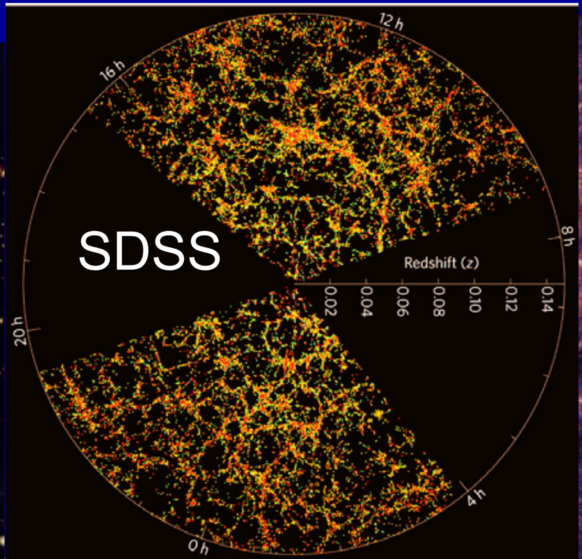

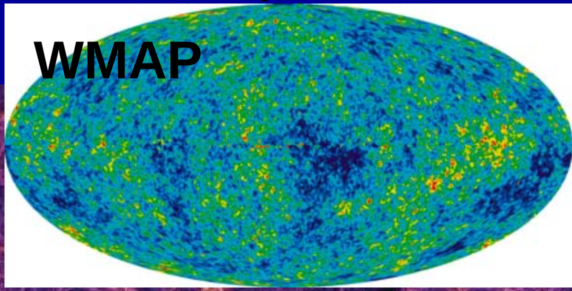

Observed Matter P(k) vs. LCDM

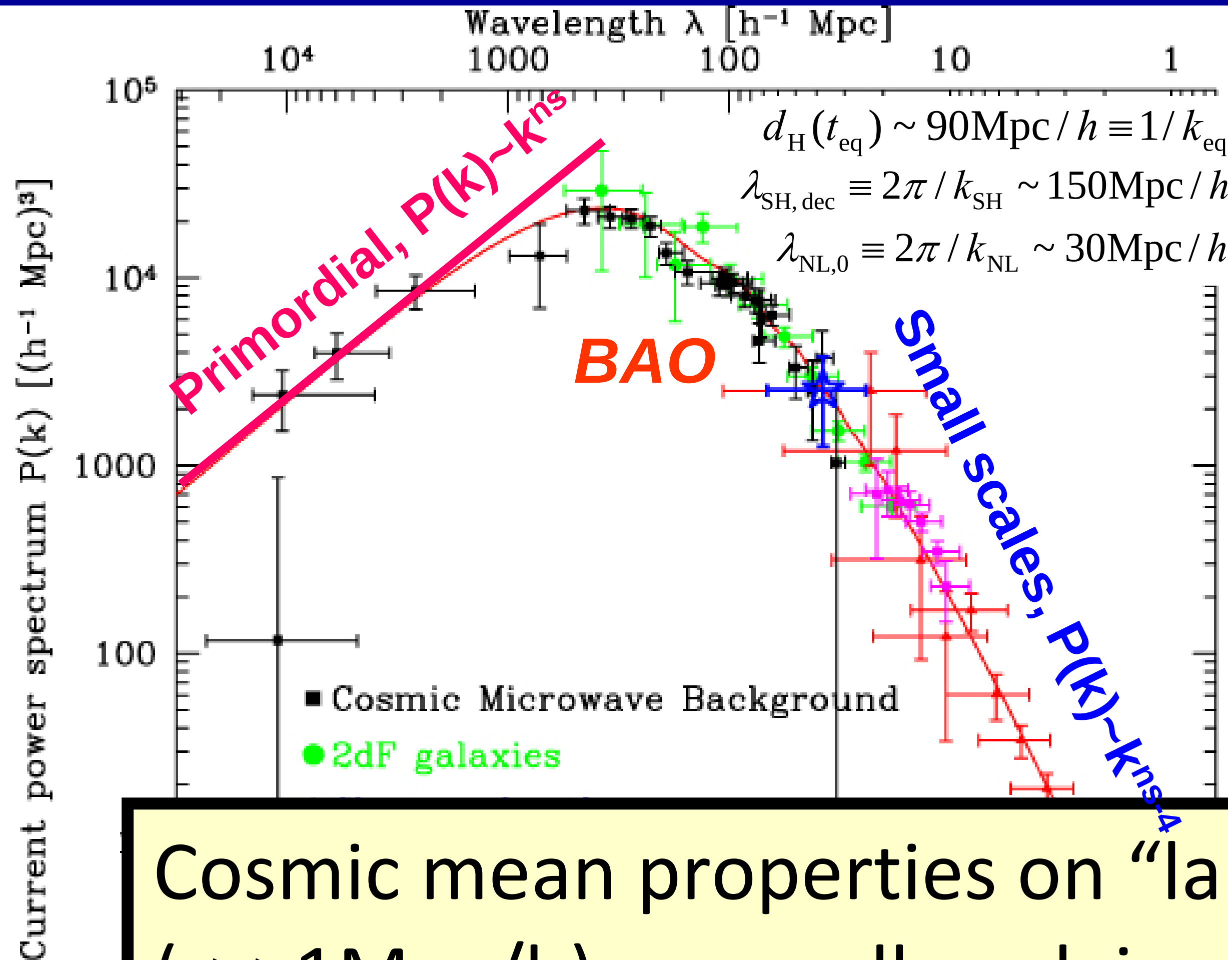

Tegmark & Zaldarriaga 2002

$P(k) \propto k^{n_s}$ with $n_s \sim 1$
(n_s=1: Harrison-Zel'dovich spectrum)
@ $k \ll k_{eq} \sim 0.01h$/Mpc

Turn-over @ $k \sim k_{eq}$

$P(k) \propto k^{(n_s-4)}$ @ $k \gg k_{eq}$
due to decay of $\Phi(k)$ on sub-horizon scales in the radiation era

...on

Nonlinear @ high-k modes,
$k > k_{NL} \sim 0.2h$/Mpc at z=0

Cosmic mean properties on "large scales" (r>>1Mpc/h) are well explained by ΛCDM.
How about nonlinear scales (<1-10Mpc/h)?

Structure Growth: *Gravitational Instability*

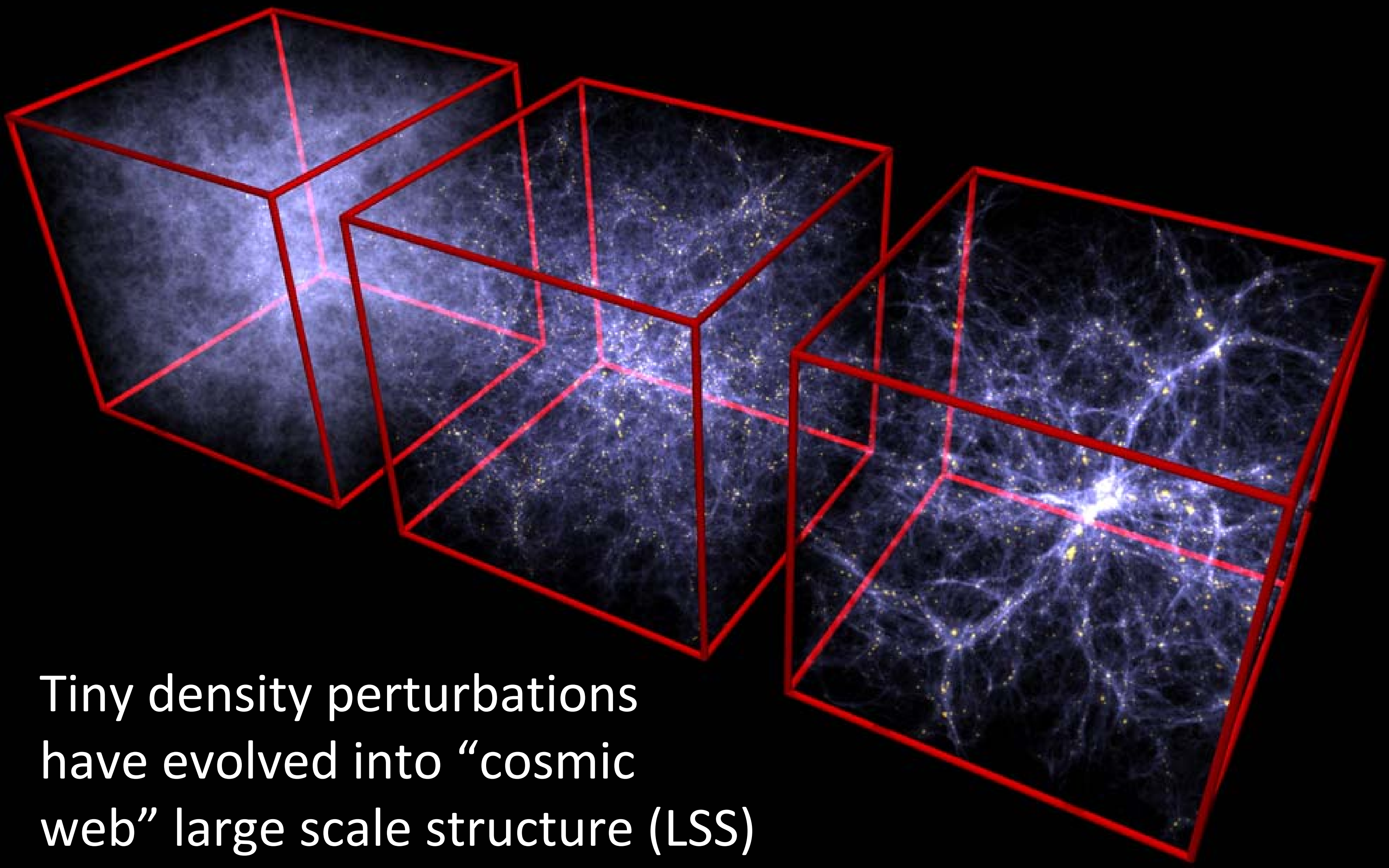

Tiny density perturbations have evolved into "cosmic web" large scale structure (LSS)

Clusters of Galaxies

Clusters are identified as dense nodes of "Cosmic Web", being building blocks of Large Scale Structure

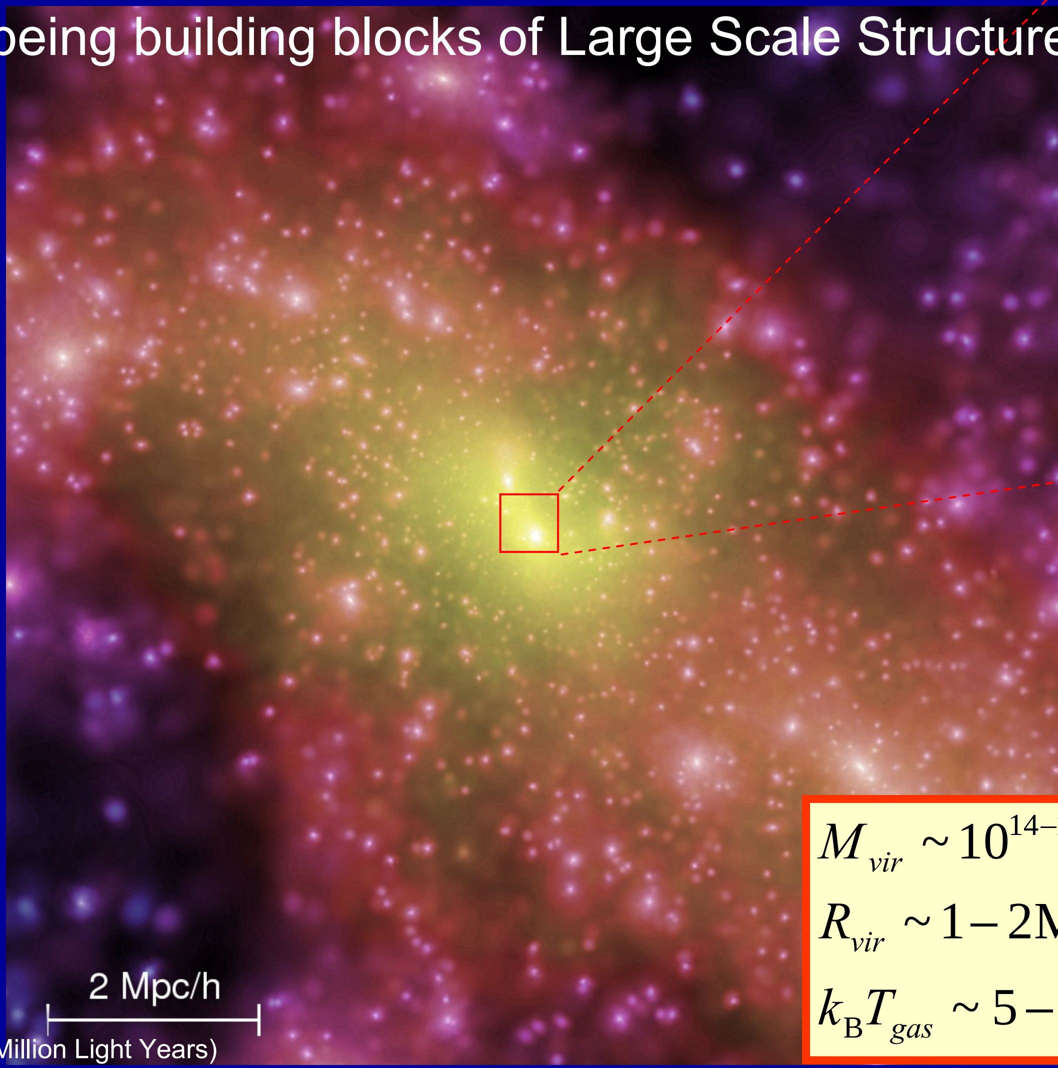

Galaxy clusters: the largest self-gravitating systems (aka, DM halos) with $\delta >> 1$, composed of $10^{2\text{-}3}$ galaxies.

$$M_{vir} \sim 10^{14-15} M_{\rm sun} / h$$

$$R_{vir} \sim 1-2{\rm Mpc}/h \;\Rightarrow\; t_{dyn} = 3-5{\rm Gyr} < {\rm t_H}$$

$$k_{\rm B} T_{gas} \sim 5-10{\rm keV}$$

Simulation of DM around a forming cluster (Springel et al. 2005, Nature, 435, 629)

Clusters as Cosmological Probes

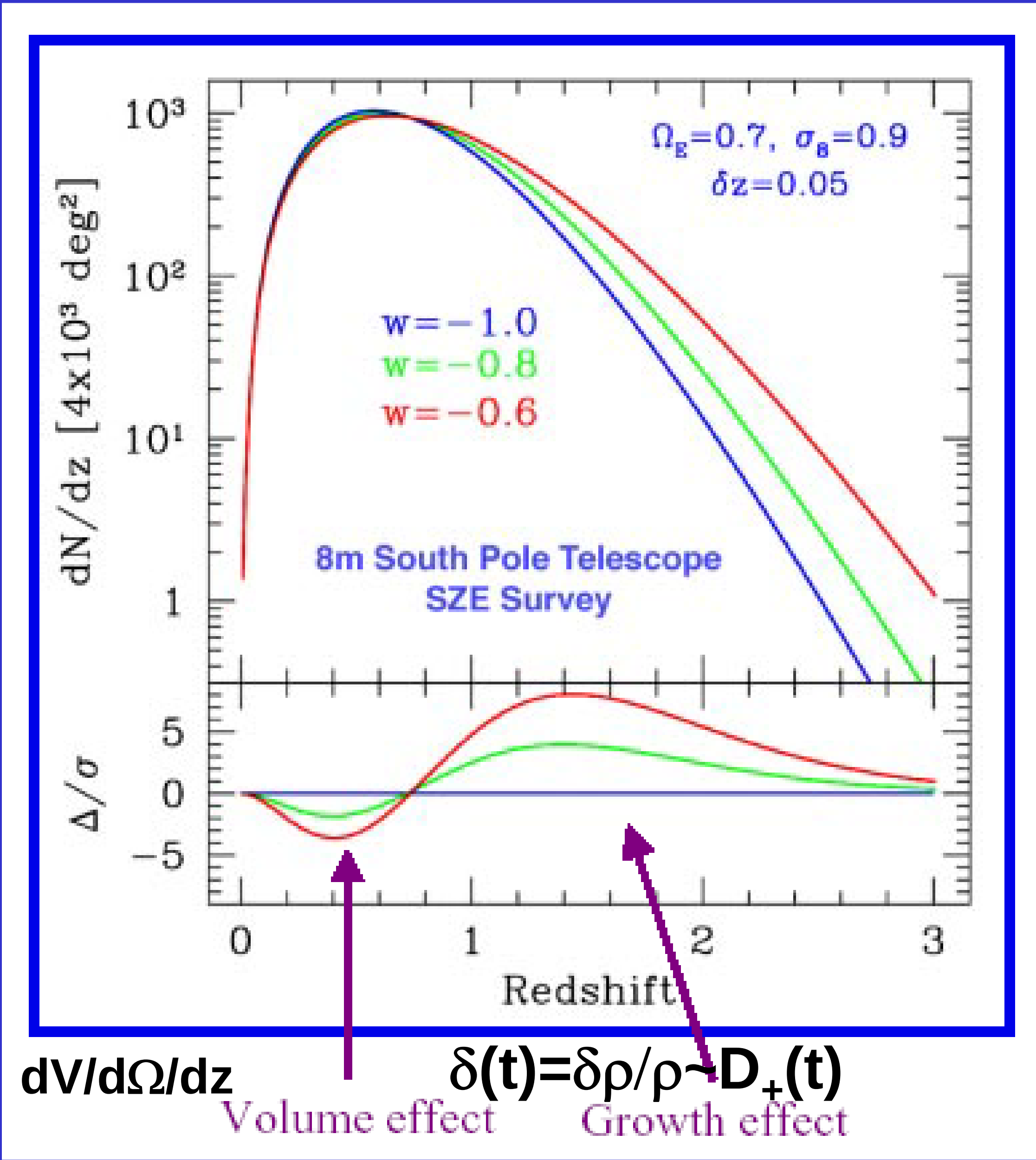

Cluster count N(z) predictions for different DE EoS, $w=P/(\rho c^2)$, normalized to the local universe

Cosmological test with structure formation in 0<z<3

Complementary to CMB observations (@z~1100)

Simulation by the SPT team

Fundamental Questions

Massive Galaxy clusters as sensitive cosmological probes:

1) **(Pseudo) Equilibrium DM halo mass profile shapes:**

   "How the shape of a cluster's DM potential depends on cluster mass and redshfit?"

2) **DM and Baryons:**

   "How the baryons distribute within the gravitational potential wells of clusters?"

3) **DM and Dark Energy (DE):**

   "How the number of clusters of a given mass should increase with time? How its growth rate depends on the background cosmology?"

4) **Primordial non-Gaussianity:**

   "What is the degree of non-Gaussianity in primordial density fluctuations?"

Compare complementary cluster observations with testable predictions of models of structure formation

Mass Profile Shapes of CDM Halos

***Empirical description of Cold Dark Matter (CDM) halos in cosmological N-body simulations*: "Navarro-Frenk-White" (NFW) universal density profile**

—Continuously steepening density profile with radius: central cusp slope of n(r) = –dlnρ/dlnr = 1 – 1.5 (cuspy but shallower than the isothermal body, n=2), asymptotic outer slope of n(r)→3

— It fits simulated DM halos that span ~9 orders of magnitude in mass (dwarf galaxies to clusters), insensitive to the initial conditions and background cosmology.

$$\rho(r)/\rho_s = (r/r_s)^{-1}(1+r/r_s)^{-2}$$

$$c_{vir} := r_{vir}/r_s$$

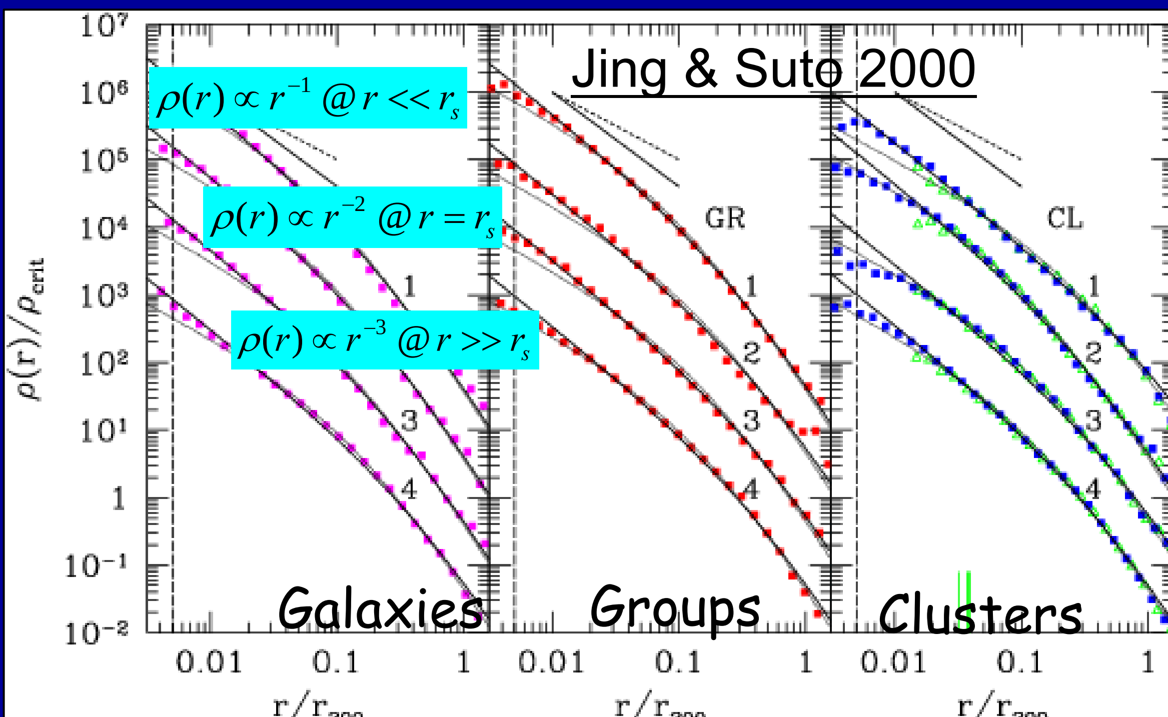

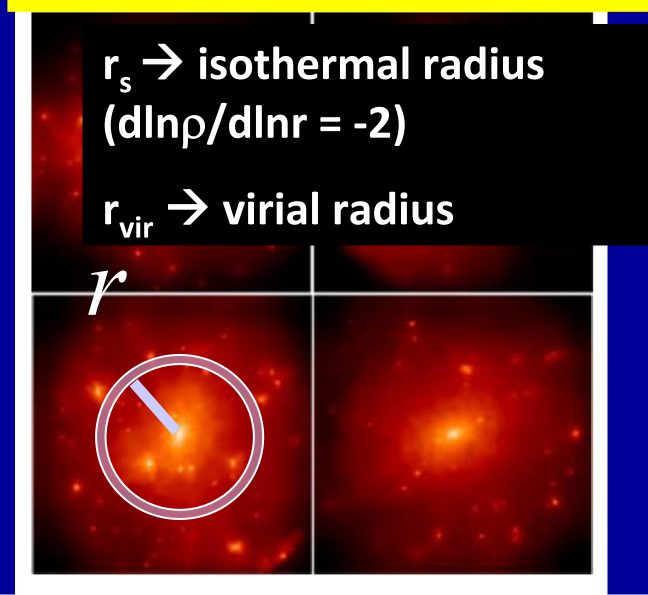

Halo Concentration-Mass (C-M) Relation

C-M relation of N-body CDM halos in the WMAP5 cosmology (σ_8=0.8)

$$\langle c_{\rm vir} \rangle = c_0 (1+z)^{-\alpha} \left(\frac{M_{\rm vir}}{10^{15} M_{\rm sun}/h} \right)^{-\beta}$$

Duffy et al. 2008, MNRAS, 390, 64: $C_0 \sim 5.2$, $\alpha \sim 0.66$, $\beta \sim 0.084$

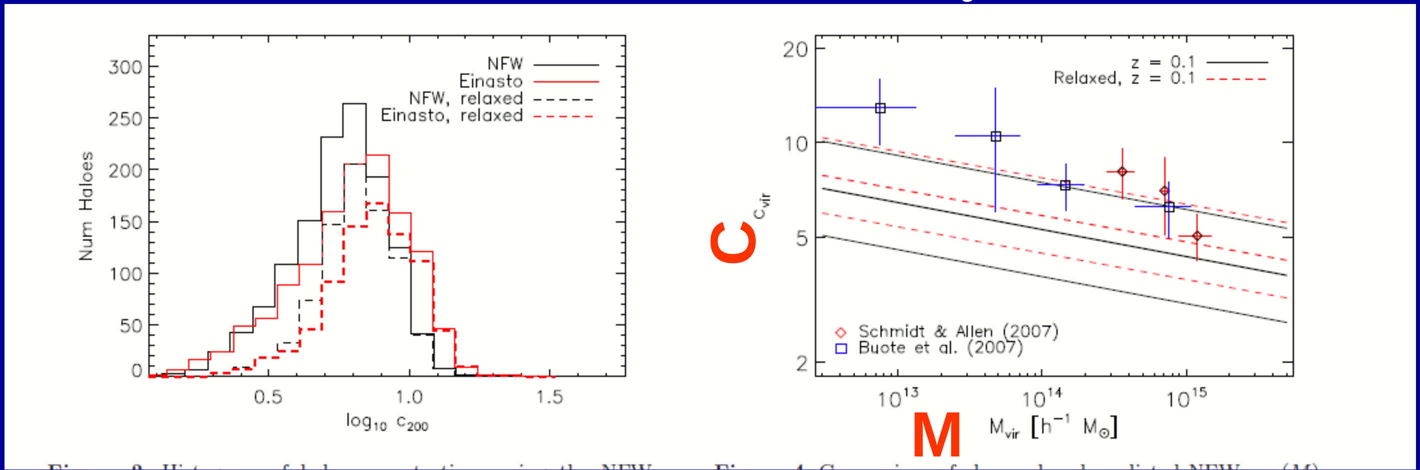

Halo concentration, c_{vir},=r_{vir}/r_s **(>1)**: **indicator of halo formation epoch**

- In a hierarchical scenario, the smaller the object, the earlier its formation epoch.
- The cosmic mean density $\rho_{m0}(1+z)^3$ is higher in earlier epochs, so that c_{vir} is correspondingly larger, on average, for less massive DM halos.
- For massive cluster-sized DM halos, lower mass concentrations are expected, so that the curvature in the mass profile shapes is pronounced – good for observations!!

2. Gravitational Lensing

Gravitationally-lensed images of background galaxies carry the imprint of $\Phi(x)$ of intervening cosmic structures:

Observable weak shape distortions can be used to derive the distribution of matter (i.e., mass) in a model independent way!!

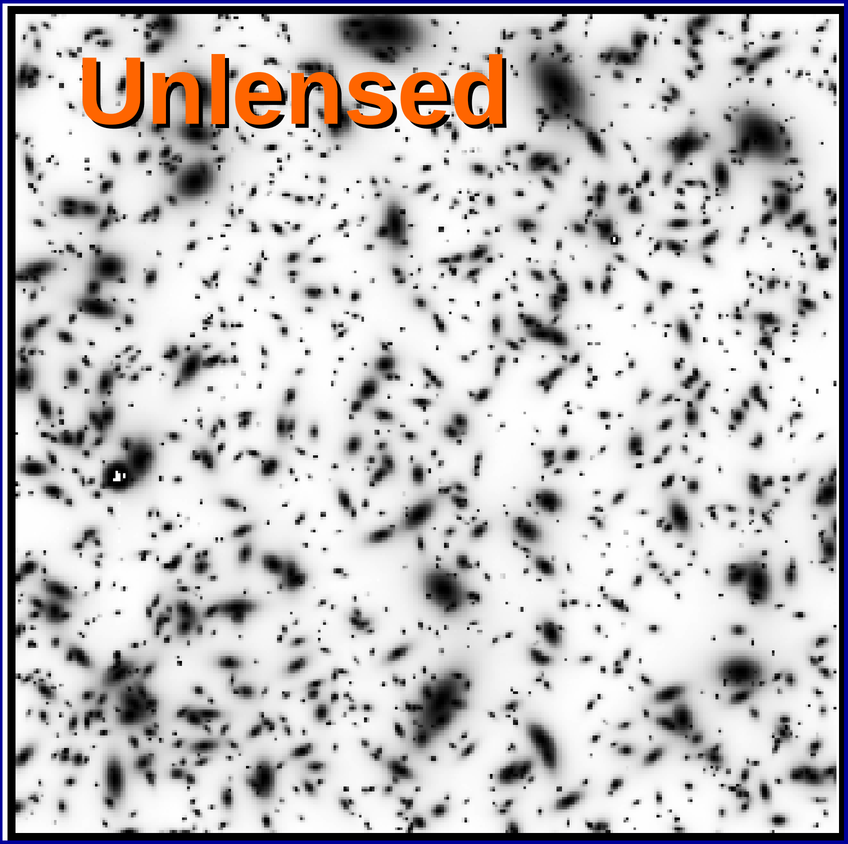

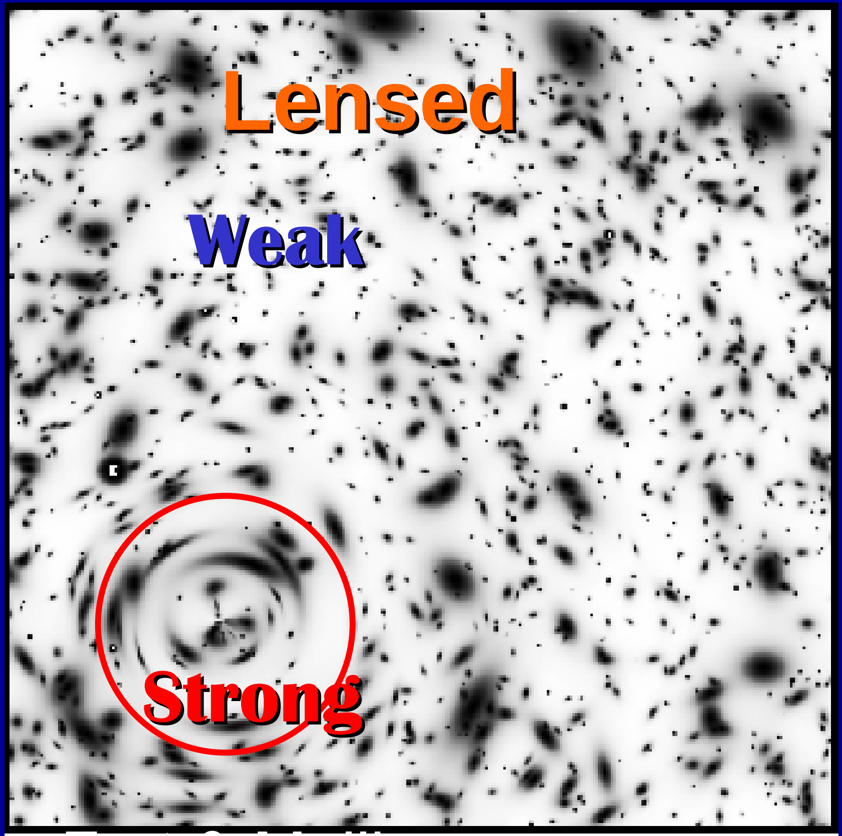

Fort & Mellier

Deflection Field: Gravitational Bending of Light Rays

Gravitational deflection angle in the weak-field limit (|Φ|/c^2<<1)

Light rays propagating in an inhomogeneous universe will undergo **small transverse excursions** along the photon path: i.e., **light deflections**

Bending angle

$$\delta\hat{\alpha} \approx \frac{\delta p_\perp}{p_\parallel} = -\frac{2}{c^2}\nabla_\perp \Psi(x_\parallel, x_\perp)\delta x_\parallel$$

Small transverse excursion of photon momentum

$$\hat{\alpha}^{\mathrm{GR}} = 2\hat{\alpha}^{\mathrm{Newton}} \rightarrow \frac{4GM}{c^2 r} = 1.''75\left(\frac{M}{M_{sun}}\right)\left(\frac{r}{R_{sun}}\right)^{-1}$$

Lens Equation

Lens equation **(Cosmological lens eq. + single/thin-lens approx.)**

β: true (but unknown) source position

θ: apparent image position

$$\boldsymbol{\beta} - \boldsymbol{\theta} = \frac{D_{LS}}{D_{OS}} \int \delta\hat{\boldsymbol{\alpha}}(\boldsymbol{\theta}) \equiv \boldsymbol{\alpha}(\boldsymbol{\theta})$$

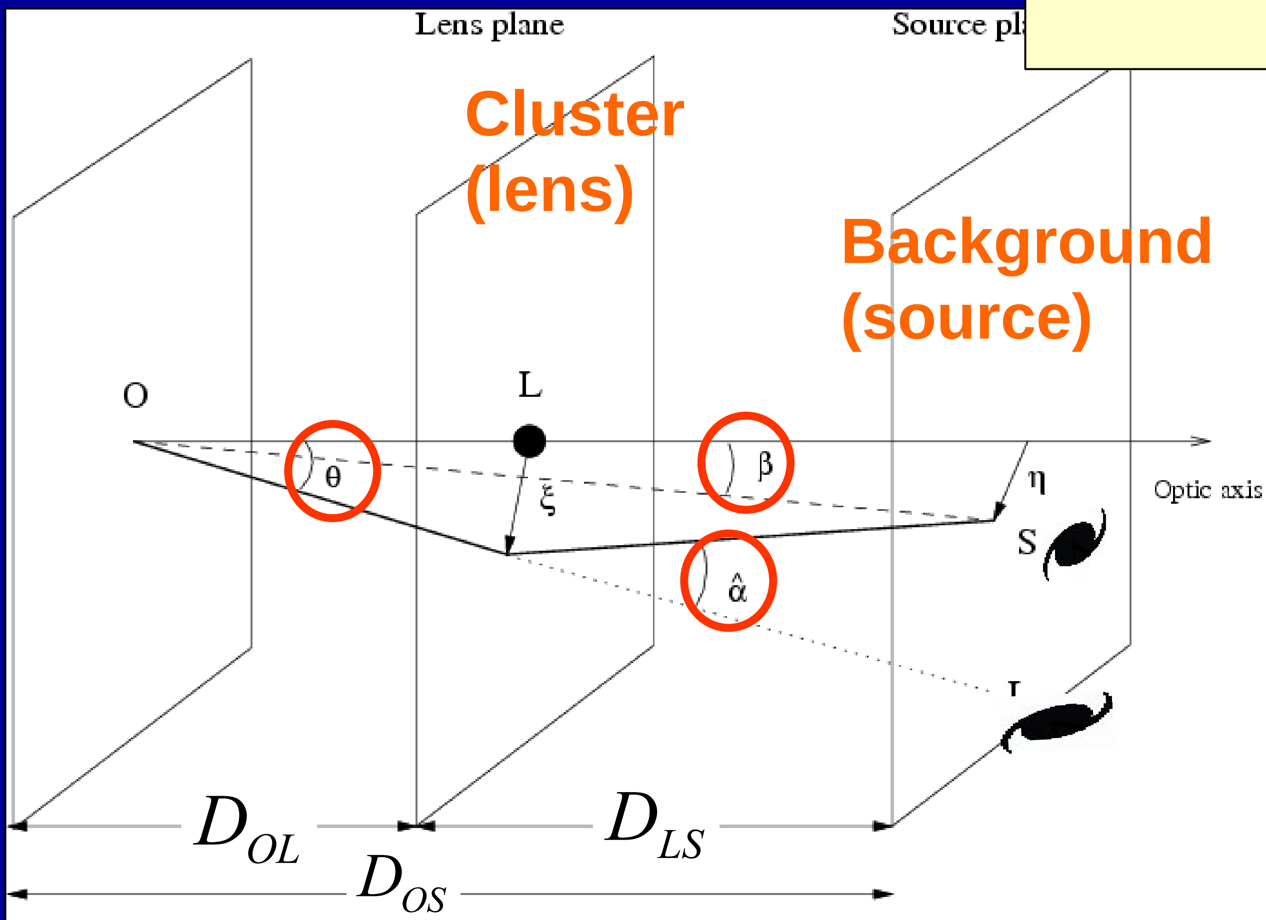

Poisson eq (2D):

div $\alpha = \nabla \cdot \alpha \equiv 2\kappa$

with $\kappa(\theta) \propto \Sigma(\theta)$

D_{OL}, D_{LS}, $D_{OS} \sim O(c/H_0)$

For a rigid derivation of cosmological lens eq., see, e.g., Futamase 95

Strong and Weak Regimes in Cluster Gravitational Lensing

- **Strong Gravitational Lensing (SL)**
- **Weak Gravitational Lensing (WL)**
  — *Tangential Shape Distortion*
  — *Magnification bias*

Se my lecture notes on

"**Cluster Weak Gravitational Lensing**"

from the "International School of Physics Enrico Fermi 2008, Italy" (also found at the Net Advance of Physics) arXiv:1002.3952

Theoretical backgrounds and basic concepts on cosmological lensing and observational techniques are summarized in these lecture notes.

Strong Lensing

Strong-lensing phenomena include: **multiple imaging**, **high flux amplification**, **arc-like image features** due to gravitational light deflection of the order 1-60 arcsec in cluster cores

[Left] 33 lensed images of *11* BG galaxies identified in HST/ACS/NIC3 multiband images by SL analysis of Cl0024+17 (Zitrin, Broadhurst, Umetsu+09, MNRAS, 396, 1985)

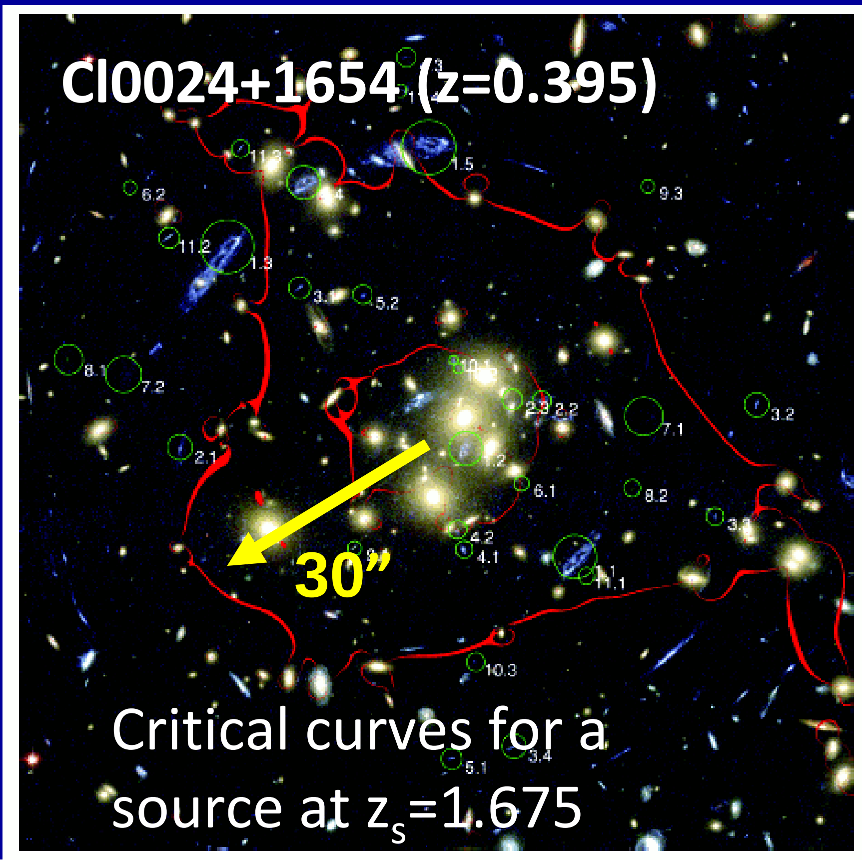

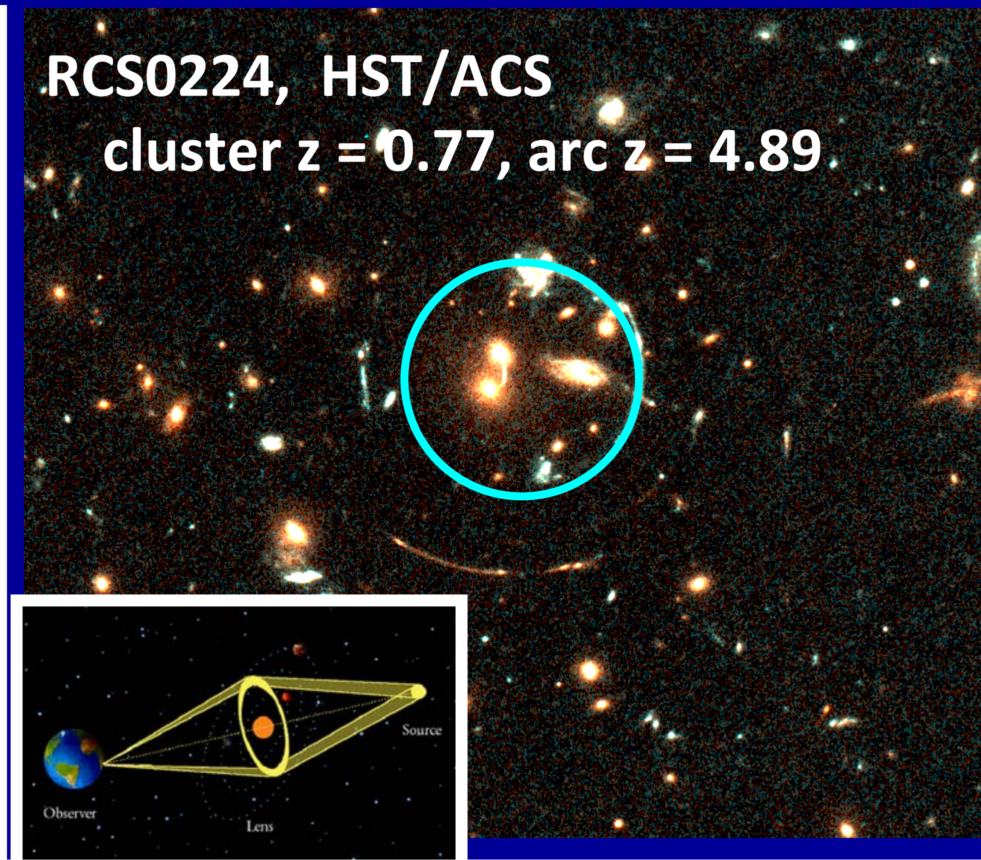

Strong Lensing to Map the Central Cluster Mass Distribution

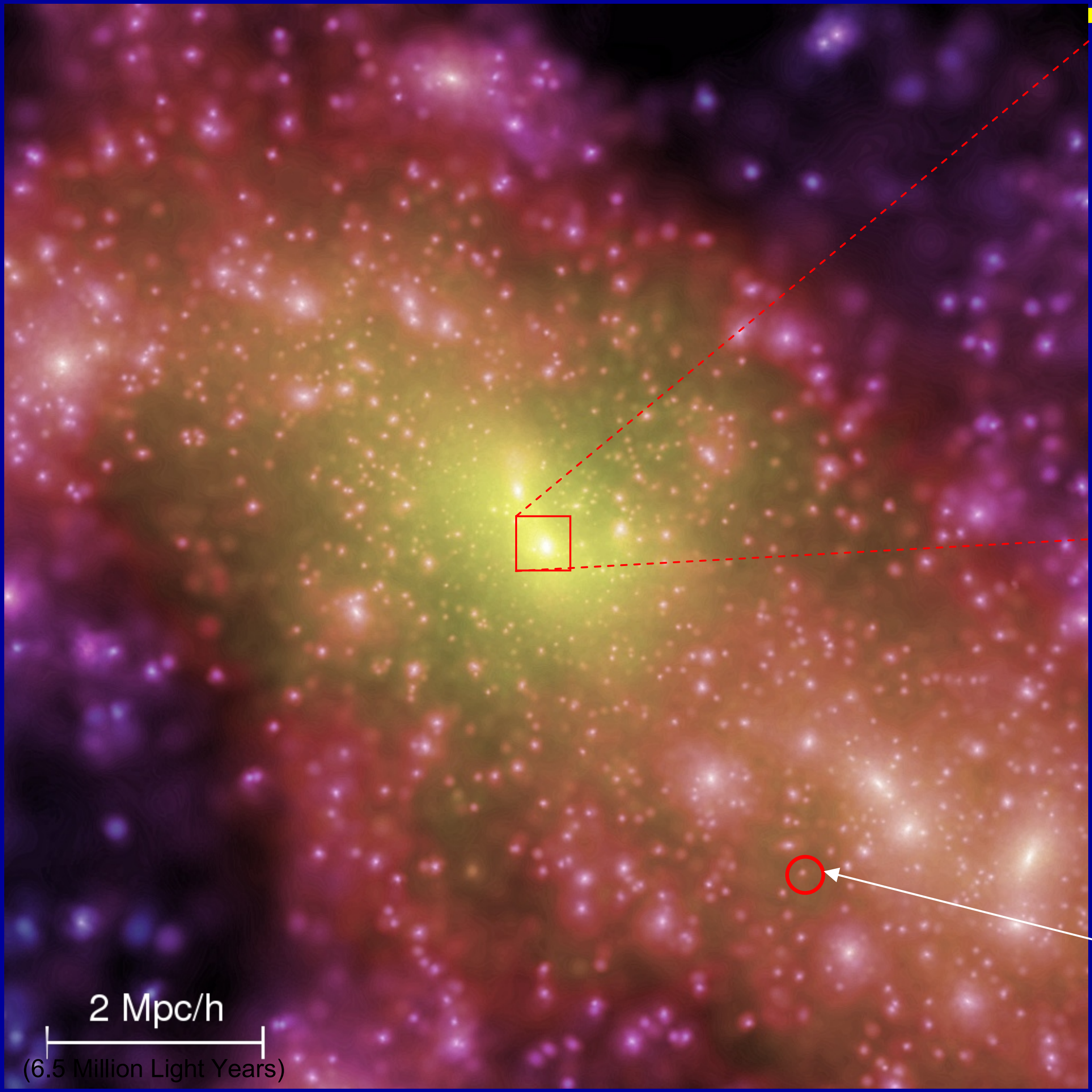

Simulation of dark matter around a forming cluster (Springel et al. 2005)

Deep HST image of massive cluster

$$R \propto \frac{\theta_{Einstein}}{\sqrt{N_{Arcs}}}$$

WHERE R IS THE RESULTING SPATIAL RESOLUTION OF THE DARK MATTER MAP

Weak Lensing [1]: Tangential Shape Distortion

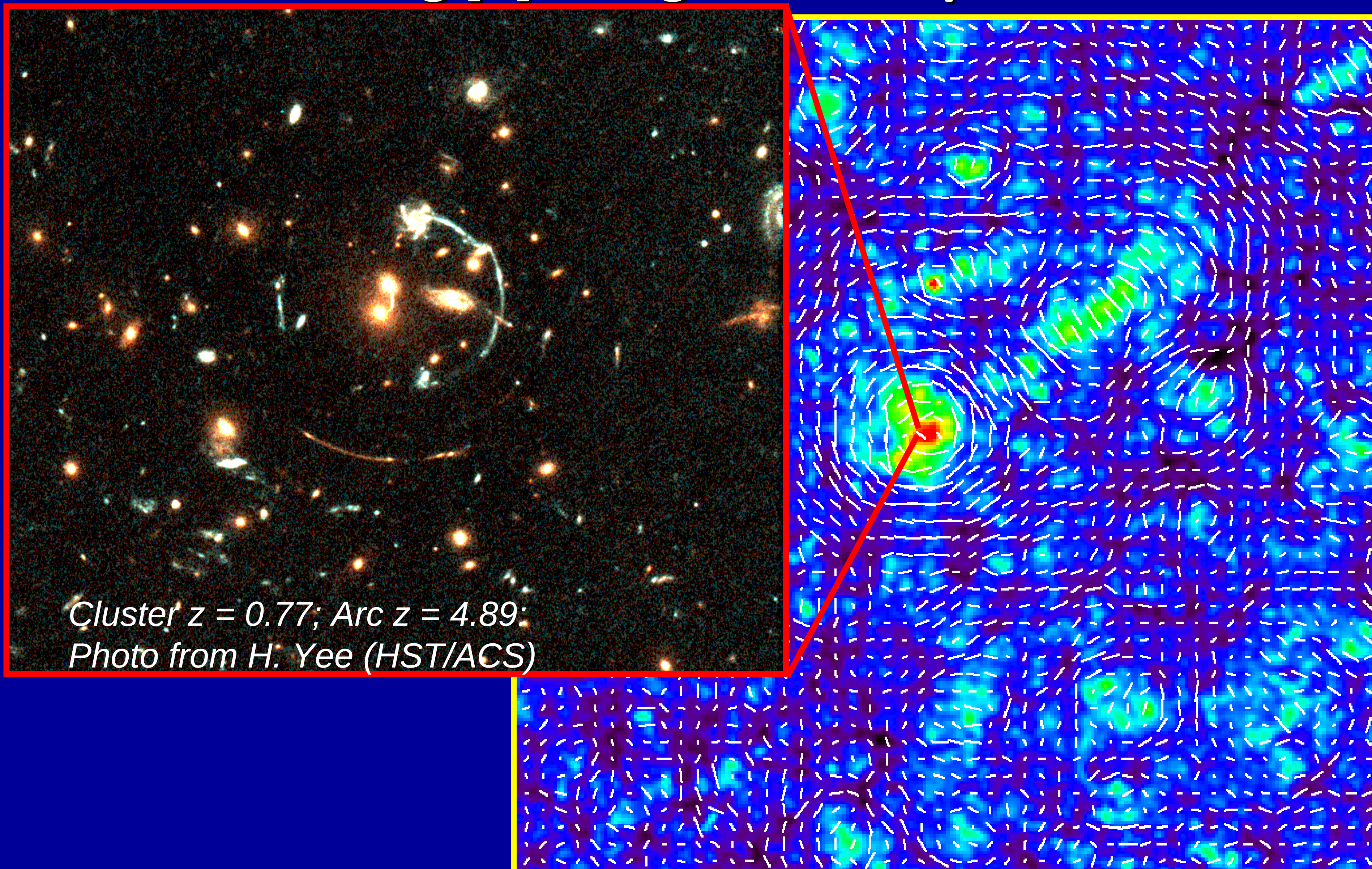

Simulated 3x3 degree field (Hamana 2002)

Tangential Distortion Profile

$$\gamma_+(r) \propto \Delta\Sigma(r) \equiv \bar{\Sigma}(<r) - \Sigma(r)$$

Measure of tangential coherence of distortions around the cluster (Tyson & Fisher 1990)

Mean tangential ellipticity of background galaxies (γ_+) as a function of cluster radius; uses typically (1-2) x 10^4 background galaxies per cluster, yielding typically S/N=5-15 per cluster.

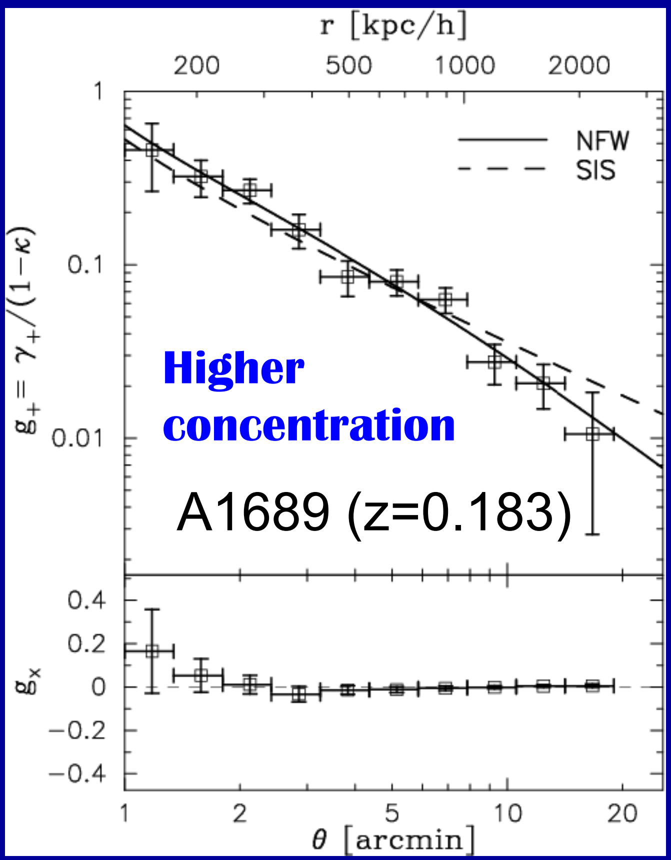

Umetsu & Broadhurst 2008, ApJ, 684 , 177

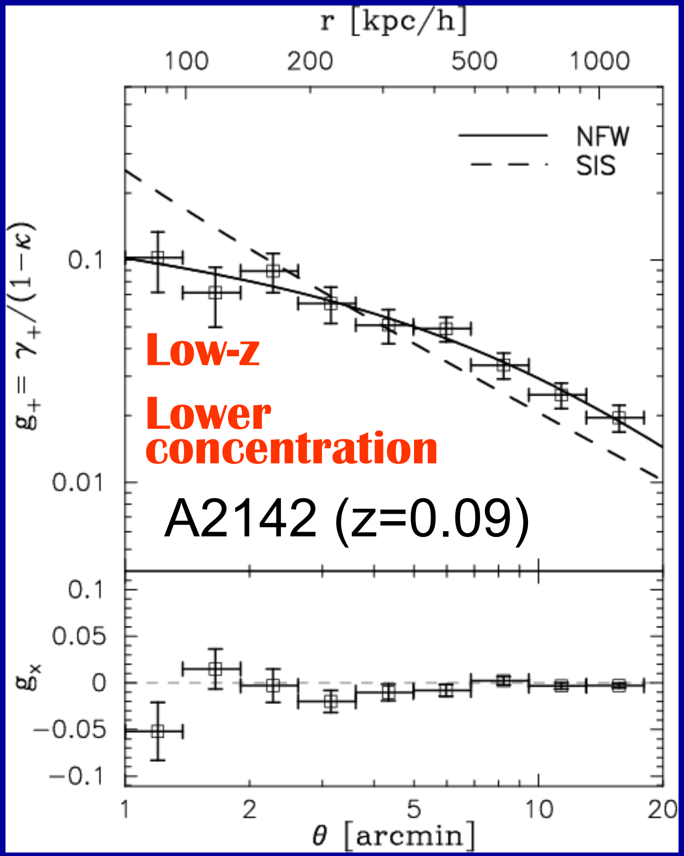

Umetsu, Birkinshaw, Liu+ 09, ApJ, 694, 1643

Mass Sheet Degeneracy

Information of "shapes" alone

canNOT fully constrain the mass distribution, allowing a one-parameter family of linear transformations that leave the observed distortion g=γ/(1-κ) unchanged:

Global invariance linear transformation

$$\kappa(\vec{\theta}) \to \lambda\kappa(\vec{\theta}) + 1 - \lambda$$

$$\gamma(\vec{\theta}) \to \lambda\gamma(\vec{\theta})$$

$$g(\vec{\theta}) \to g(\vec{\theta})$$

- In the strict weak lensing limit (γ,κ<<1), this is equivalent to adding a constant mass-sheet with 1-λ~Δκ.
- Δκ =0 can be assured when a sufficiently large sky coverage is available.

One needs to employ an additional, independent piece of information (just 1DoF) to break the degeneracy.

Weak Lensing [2]: Magnification Bias

Magnification bias: Lens-magnification induced fluctuations in the background density field (Broadhurst, Taylor, & Peacock 1995)

$$\delta n(\boldsymbol{\theta}) / n_0 = \mu^{s-1}(\boldsymbol{\theta}) - 1 \approx 2(s-1)\Sigma(\boldsymbol{\theta}) / \Sigma_{crit}$$

with unlensed flux-limited counts of background galaxies $n_0(>F) \propto F^{-s}$

When the count-slope is shallow, i.e., s<1, a net deficit of counts is expected.

Figure courtesy of Masahiro Takada

Shear vs. Magnification

Count depletion of red background galaxies in CL0024+1654 (z=0.395)

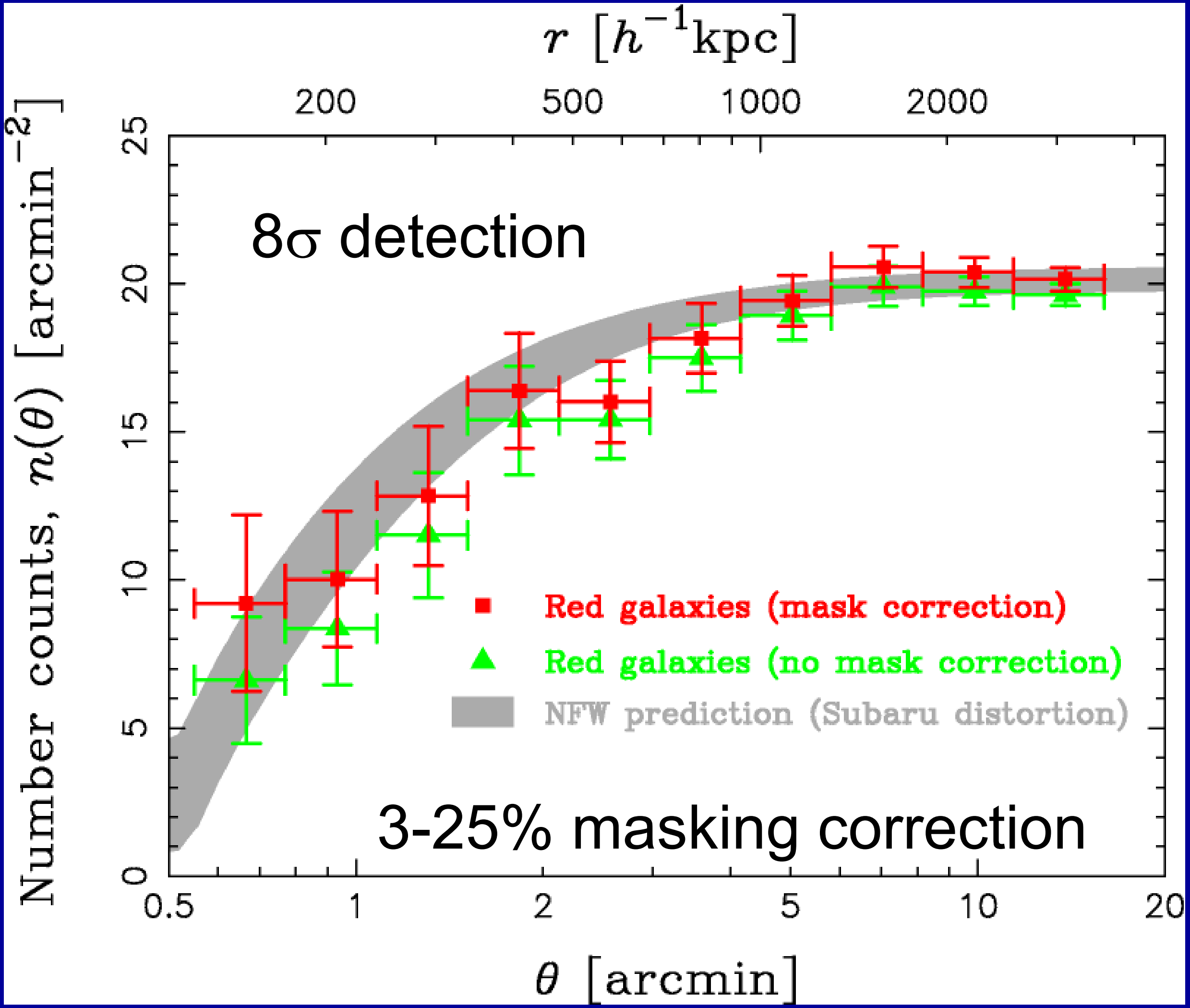

Distortion of faint background galaxies

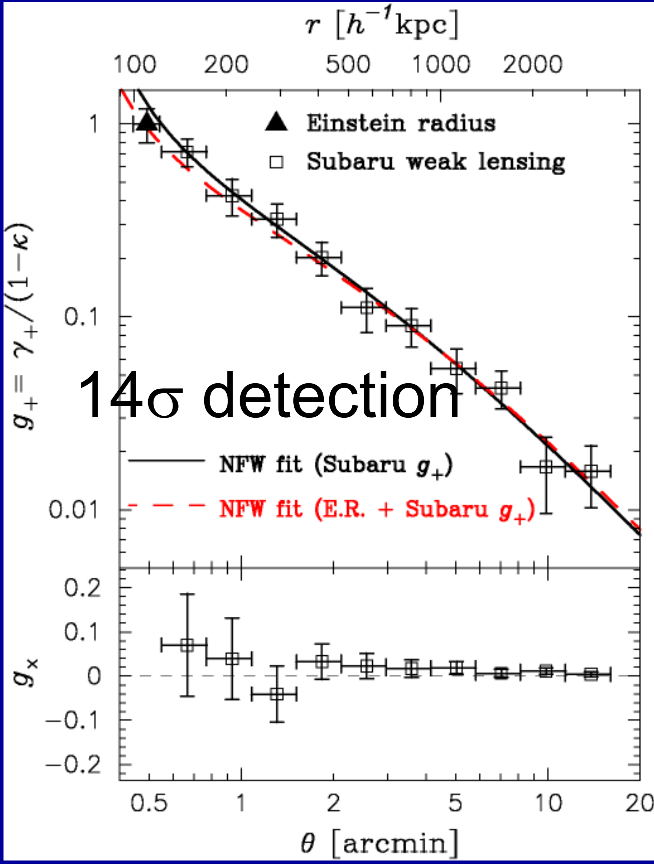

Umetsu, Medezinski, Broadhurst et al. 2010, ApJ, 714, 1470

3. Applications to Cluster Observations: Subaru and Hubble Imaging

Massive clusters (>$10^{15} M_{sun}/h$) with strong lensing phenomena

- A1689 (z=0.183)
- A1703 (z=0.281)
- A370 (z=0.375)
- Cl0024+1654 (z=0.395)
- RXJ1347 (z=0.451)

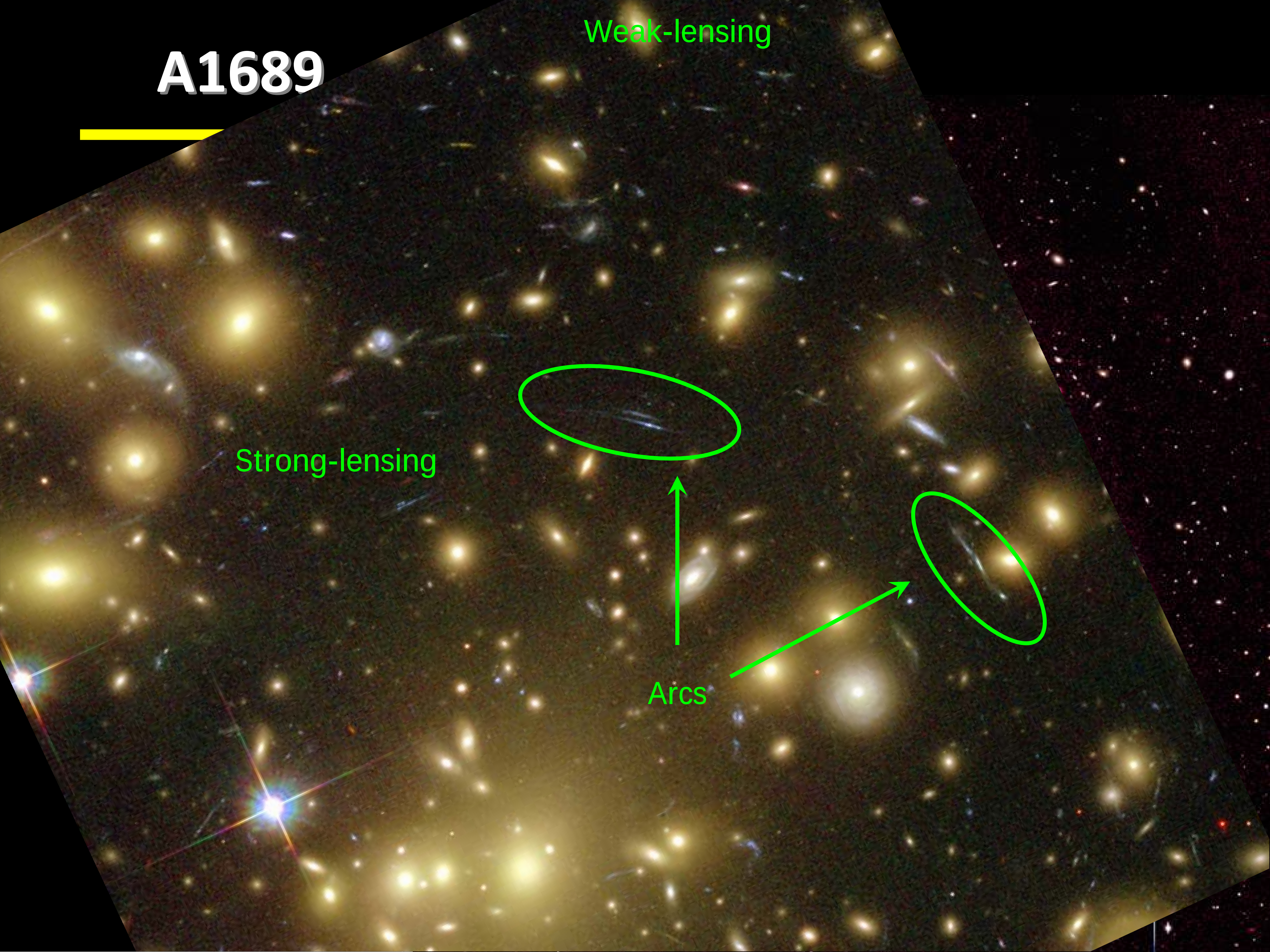
A1689
Weak-lensing
Strong-lensing
Arcs

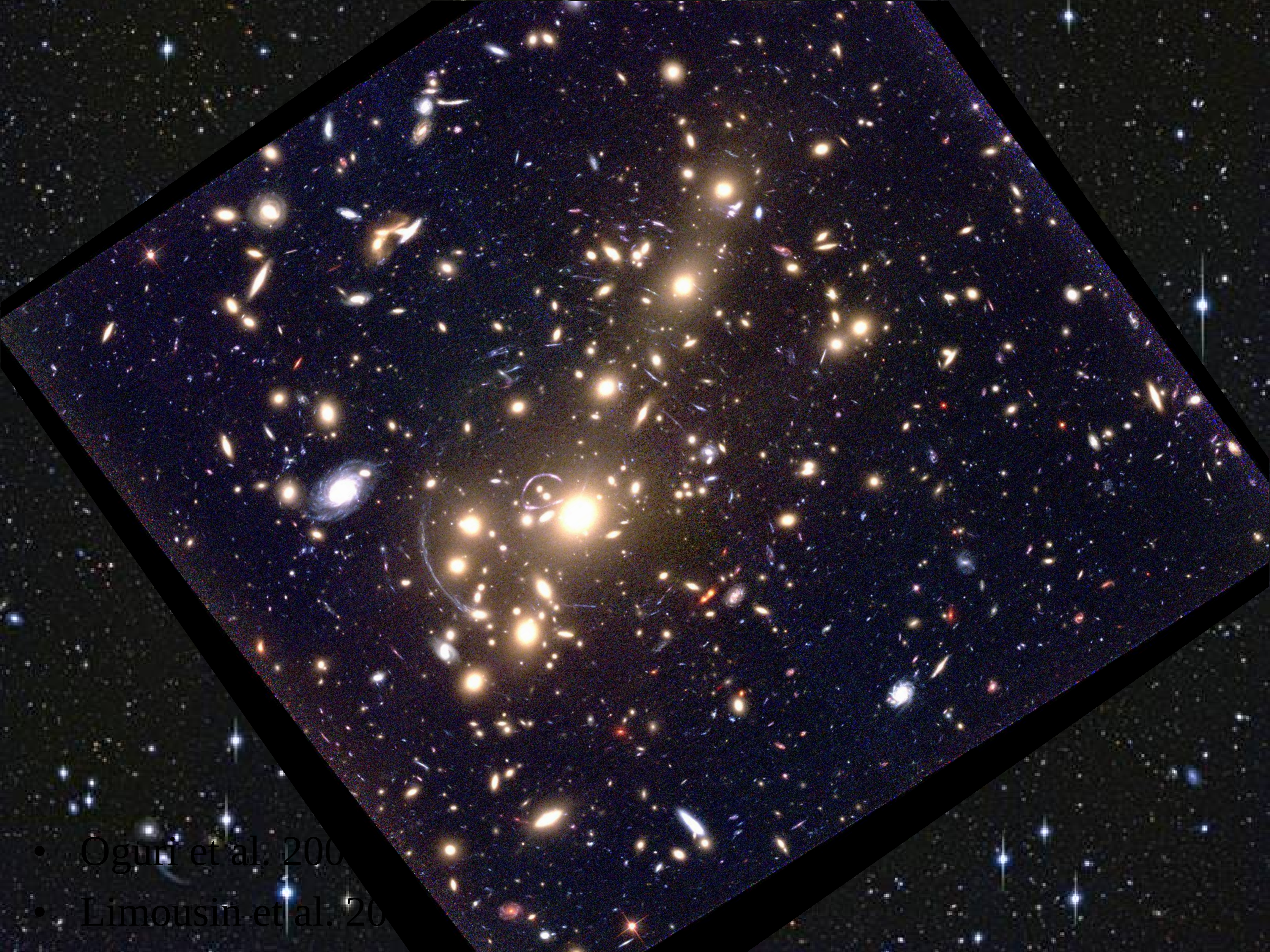

- Oguri et al. 200
- Limousin et al. 20

A37

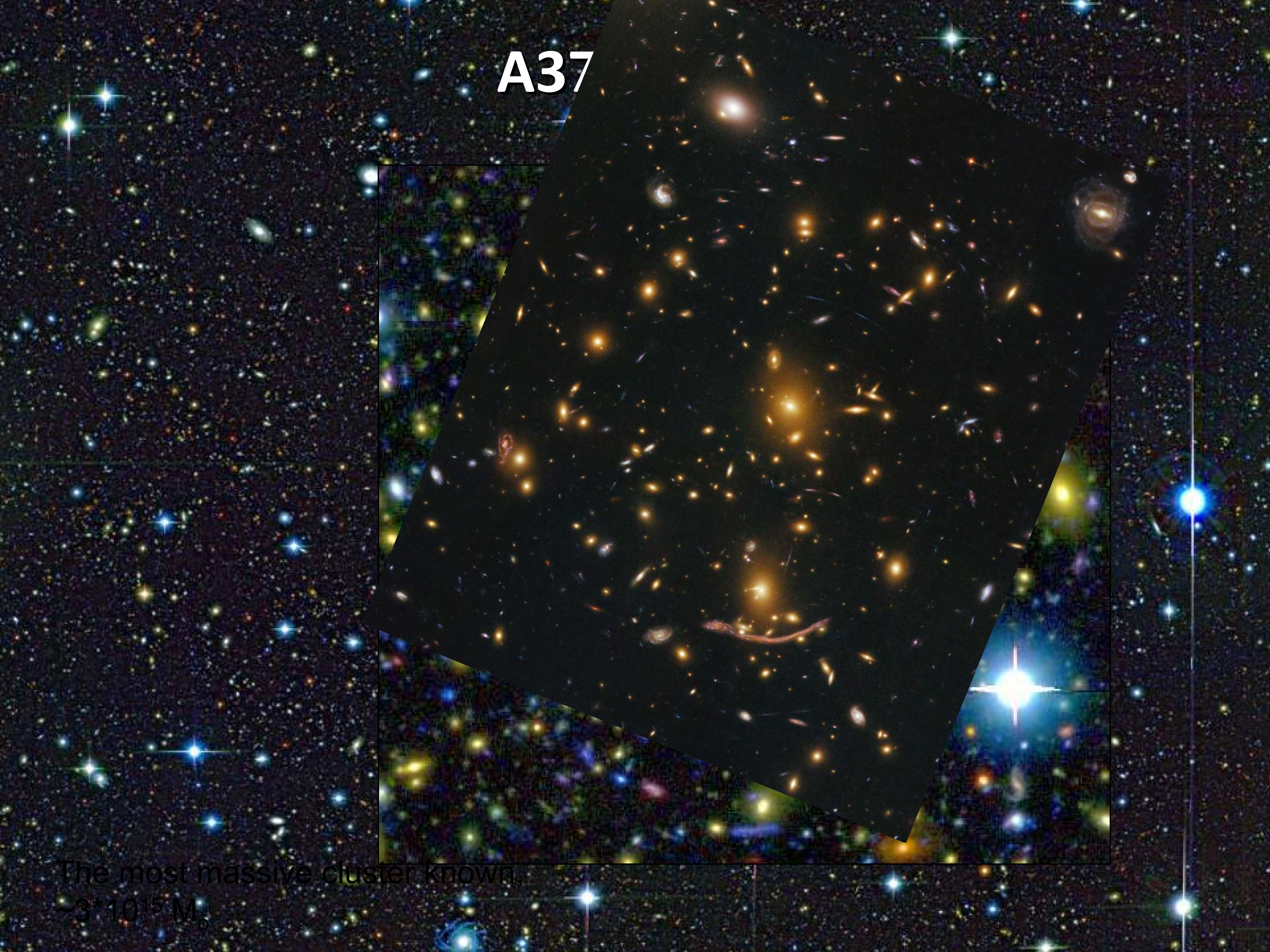

The most massive cluster known,
$\sim 3*10^{15} M_o$

Cl0024+1654 (z=0.395)

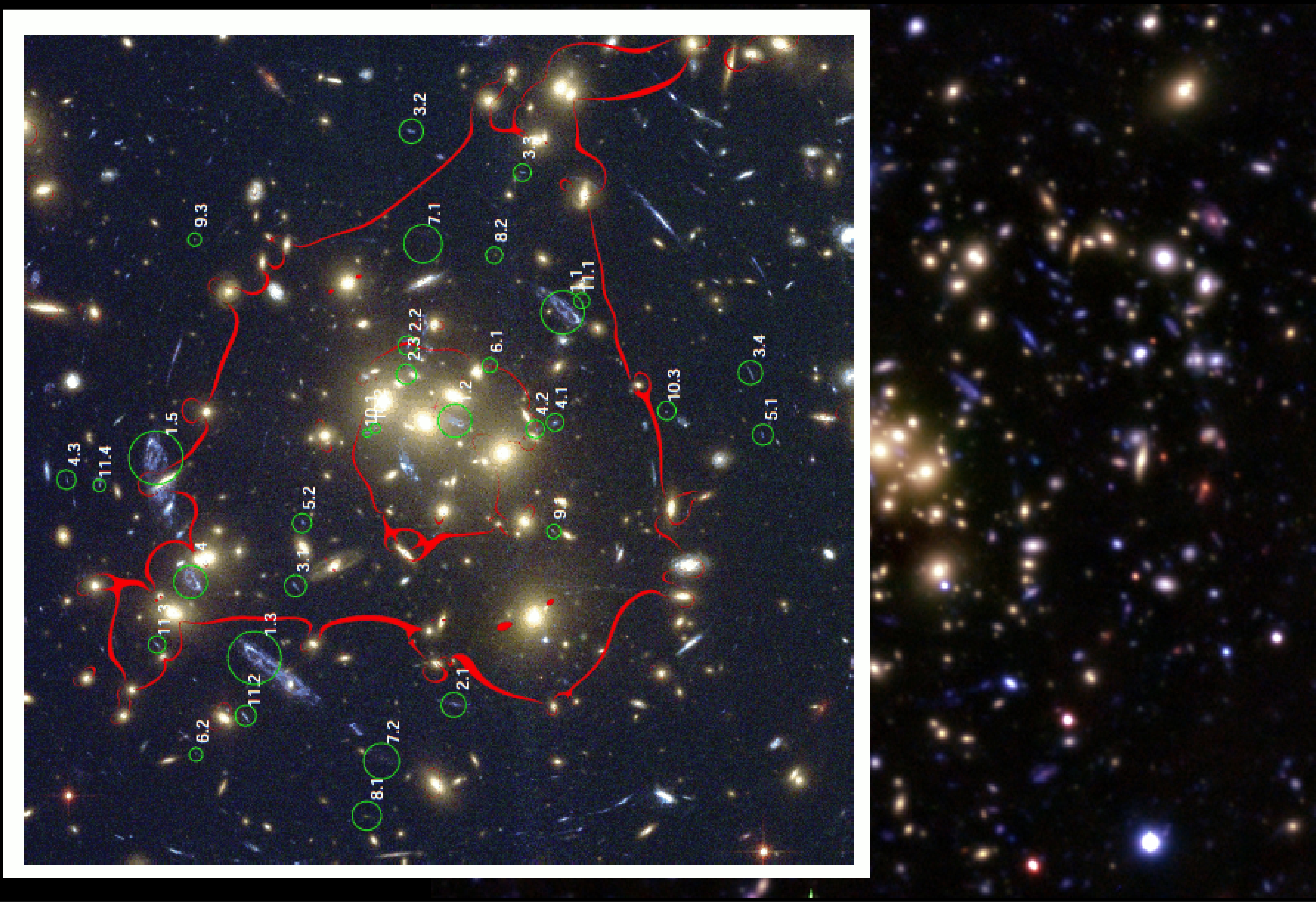

SUBARU Cluster Weak Lensing Measurements

Cl0024+17 (z=0.395)

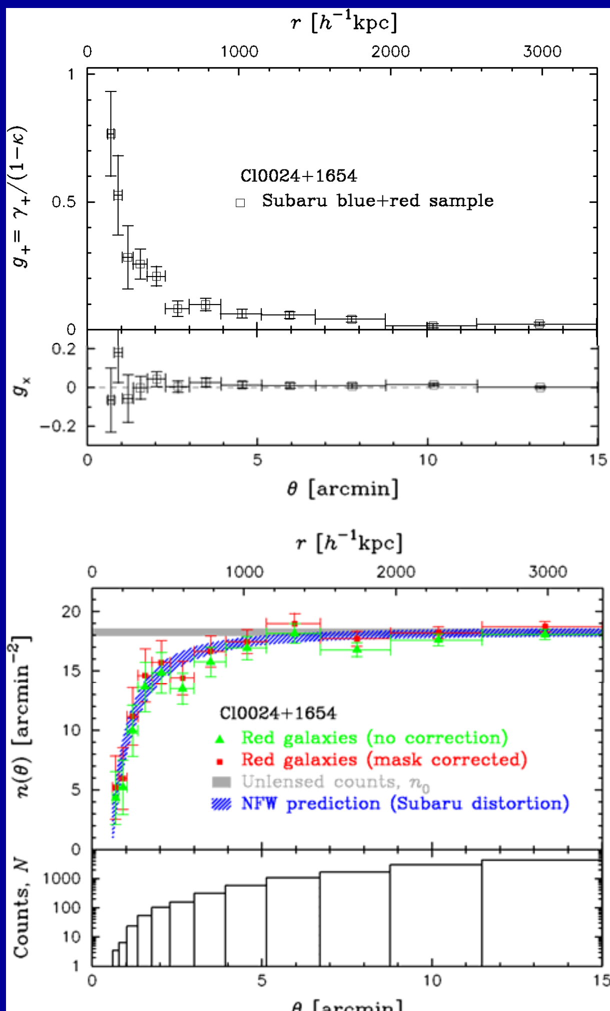

A370 (z=0.375)

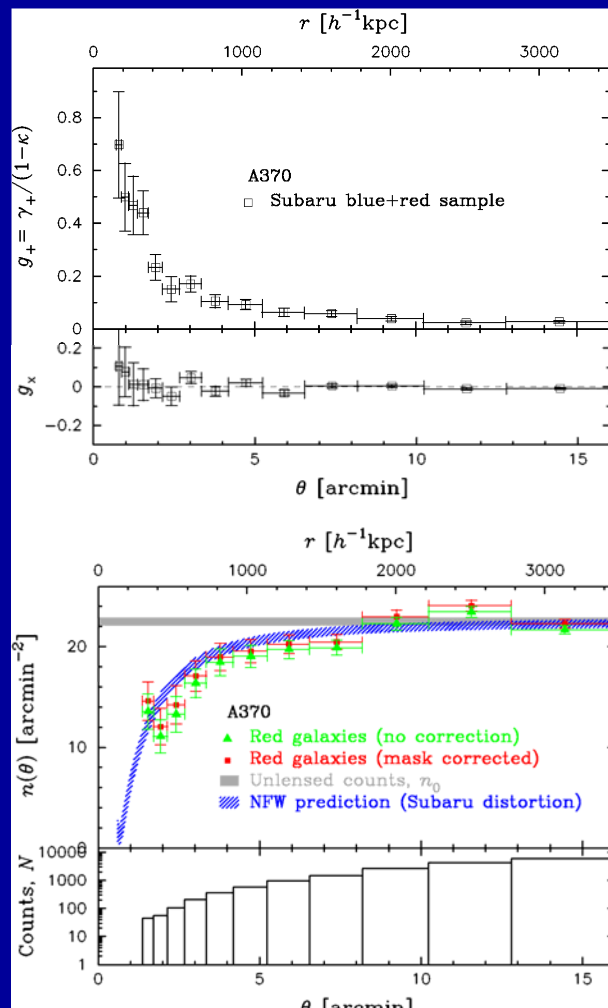

RXJ1347-11 (z=0.451)

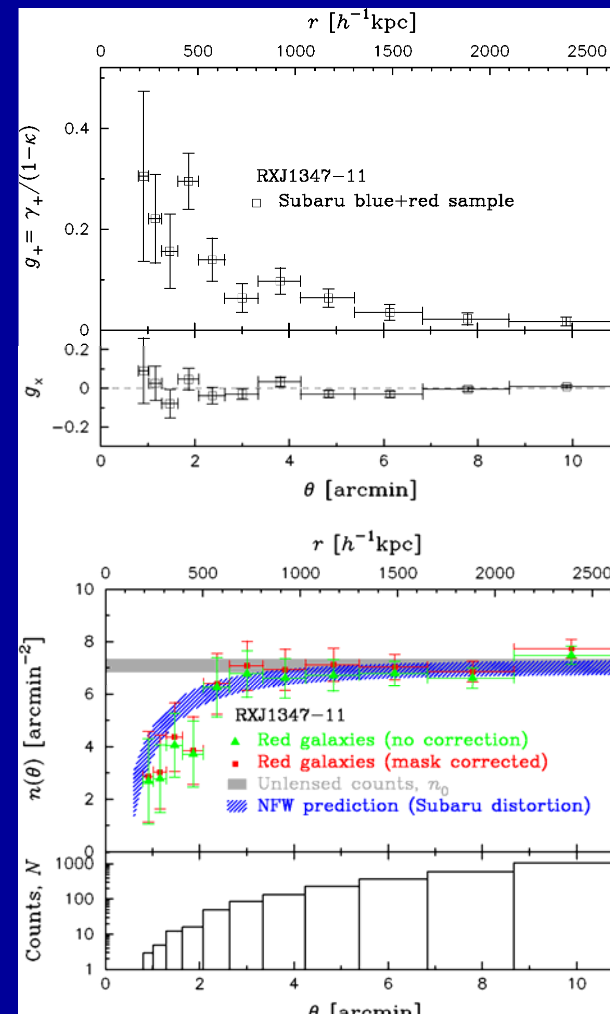

[1] Cluster Mass Profiles from Full Weak + Strong Lensing Analyses

Combining Weak (Subaru) and Strong (HST/ACS) lensing data:

→ Probing the mass density profile from 5% to 150% of the virial radius

Results for five high-mass clusters (Umetsu et al. 2010b, arXiv:1011.3044)

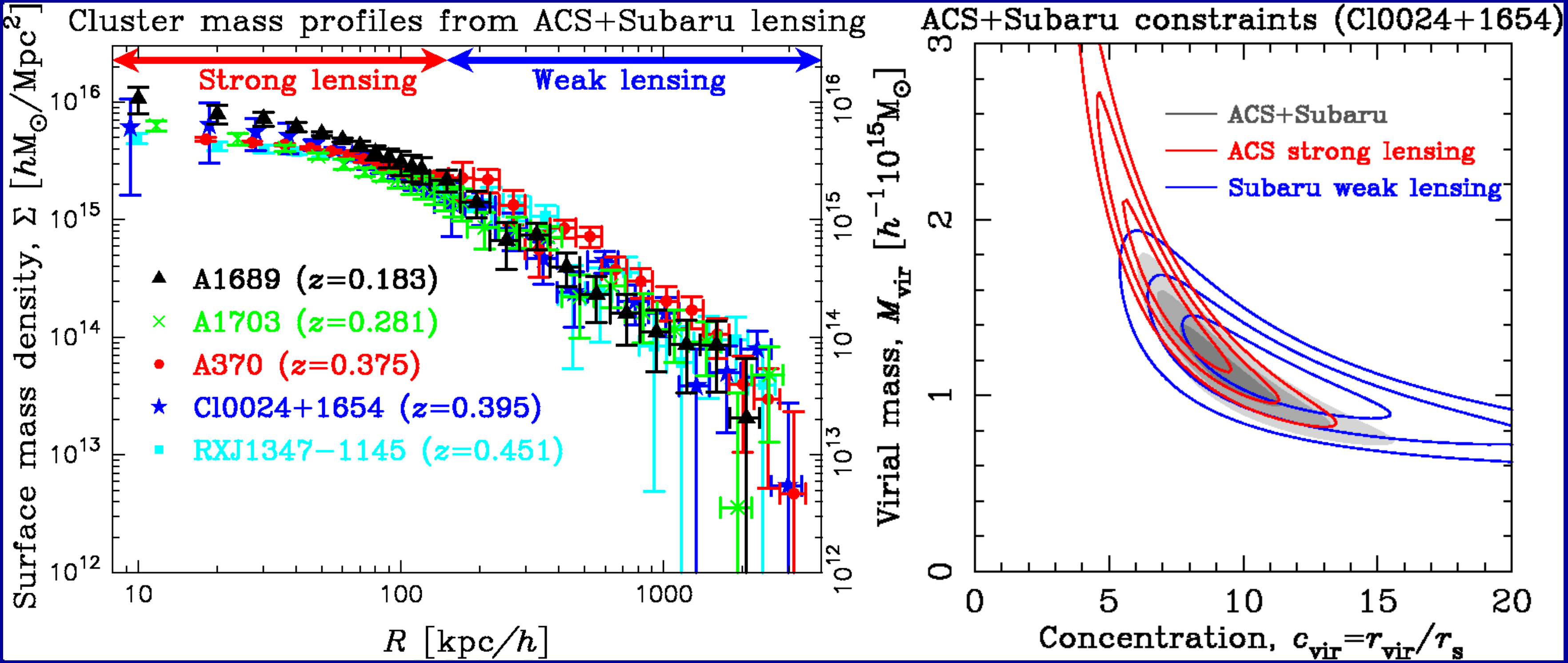

The profile shapes are consistent with CDM (NFW) over the entire cluster, but the degree of concentration appears to be higher than LCDM.

Broadhurst, Takda, Umetsu et al. 2005; Umetsu & Broadhurst 2008; Lemze et al. 2009 (A1689); Umetsu et al. 2010a (CL0024+1654); Umetsu et al. 2010b (5 clusters)

Central Density Slope (α)

TABLE 6. BEST-FIT NFW MODEL PARAMETERS **Umetsu et al. 2010b**

Cluster	NFW (weak lensing)				gNFW (weak+strong lensing)				
	M_{vir} ($10^{15} M_\odot h^{-1}$)	c_{vir}	χ^2/dof	θ_{ein}[a] ($''$)	M_{vir} ($10^{15} M_\odot h^{-1}$)	c_{-2}[b]	α	χ^2/dof	θ_{ein}[a] ($''$)
A1689	$1.266^{+0.213}_{-0.172}$	$12.92^{+3.10}_{-2.42}$	4.0/10	$48.6^{+15.4}_{-13.7}$	$1.305^{+0.193}_{-0.156}$	$13.68^{+1.19}_{-1.22}$	$0.275^{+0.413}_{-0.275}$	4.4/20	$49.7^{+12.9}_{-9.2}$
A1703	$1.253^{+0.247}_{-0.207}$	$7.08^{+2.31}_{-1.67}$	7.6/9	$28.8^{+16.1}_{-13.1}$	$1.271^{+0.227}_{-0.189}$	$7.09^{+1.06}_{-1.03}$	$0.925^{+0.191}_{-0.251}$	7.9/21	$27.8^{+14.3}_{-13.7}$
A370	$2.435^{+0.304}_{-0.258}$	$7.11^{+1.08}_{-0.92}$	9.1/13	$50.8^{+10.8}_{-9.8}$	$2.221^{+0.215}_{-0.187}$	$5.79^{+0.49}_{-0.48}$	$0.359^{+0.164}_{-0.198}$	16.4/26	$30.6^{+8.7}_{-10.0}$
Cl0024+17	$1.272^{+0.212}_{-0.184}$	$9.37^{+2.54}_{-1.87}$	12.2/11	$36.4^{+11.1}_{-10.0}$	$1.278^{+0.231}_{-0.191}$	$8.38^{+1.23}_{-1.26}$	$0.727^{+0.433}_{-0.727}$	10.8/23	$30.1^{+10.4}_{-10.3}$
RXJ1347-11	$1.479^{+0.281}_{-0.248}$	$8.42^{+2.97}_{-2.07}$	9.1/10	$40.9^{+14.0}_{-13.0}$	$1.426^{+0.113}_{-0.100}$	$7.19^{+0.43}_{-0.43}$	$0.022^{+0.210}_{-0.022}$	57.0/29	$32.6^{+4.9}_{-5.4}$

Generalized NFW (gNFW) profile w/ 3 free parameters:

$$\rho(r)/\rho_s = \frac{1}{(r/r_s)^{\alpha}(1+r/r_s)^{(3-\alpha)}}$$

$$c_{-2} := \frac{r_{vir}}{(2-\alpha)r_s}$$

Overall, shallower-than-NFW inner slopes ($\alpha<1$) are found.

Weak + strong lensing constraints on CL0024+1654 (z=0.395)

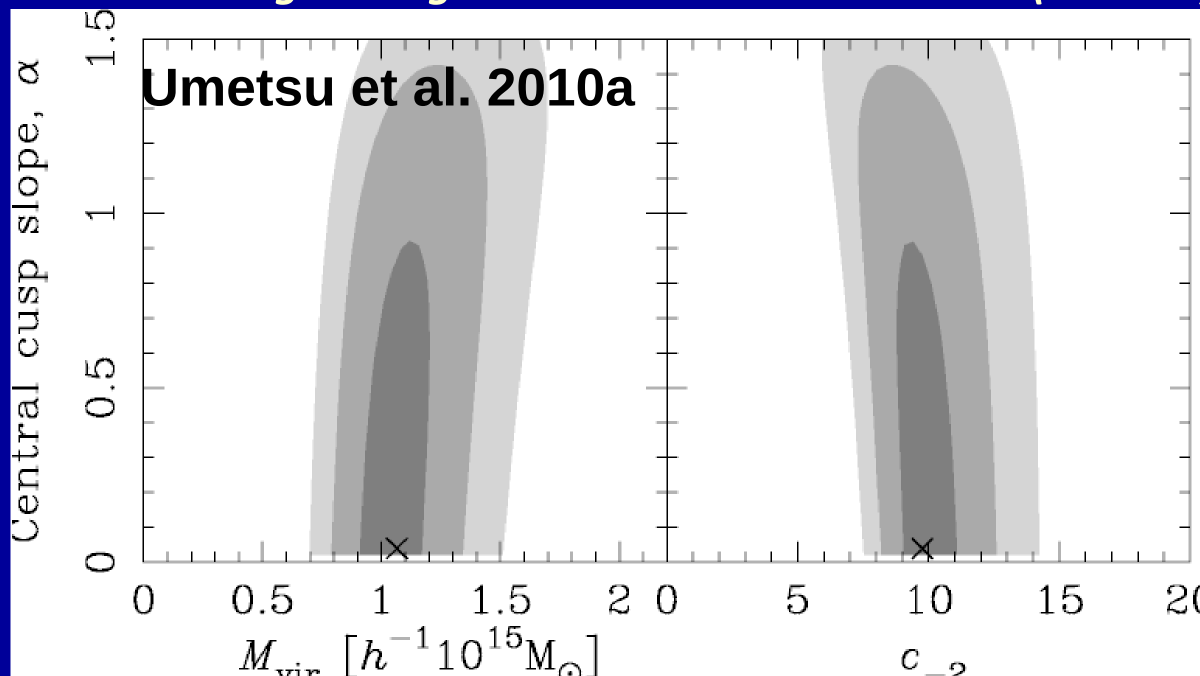

Outer Density Slopes (Weak Lensing)

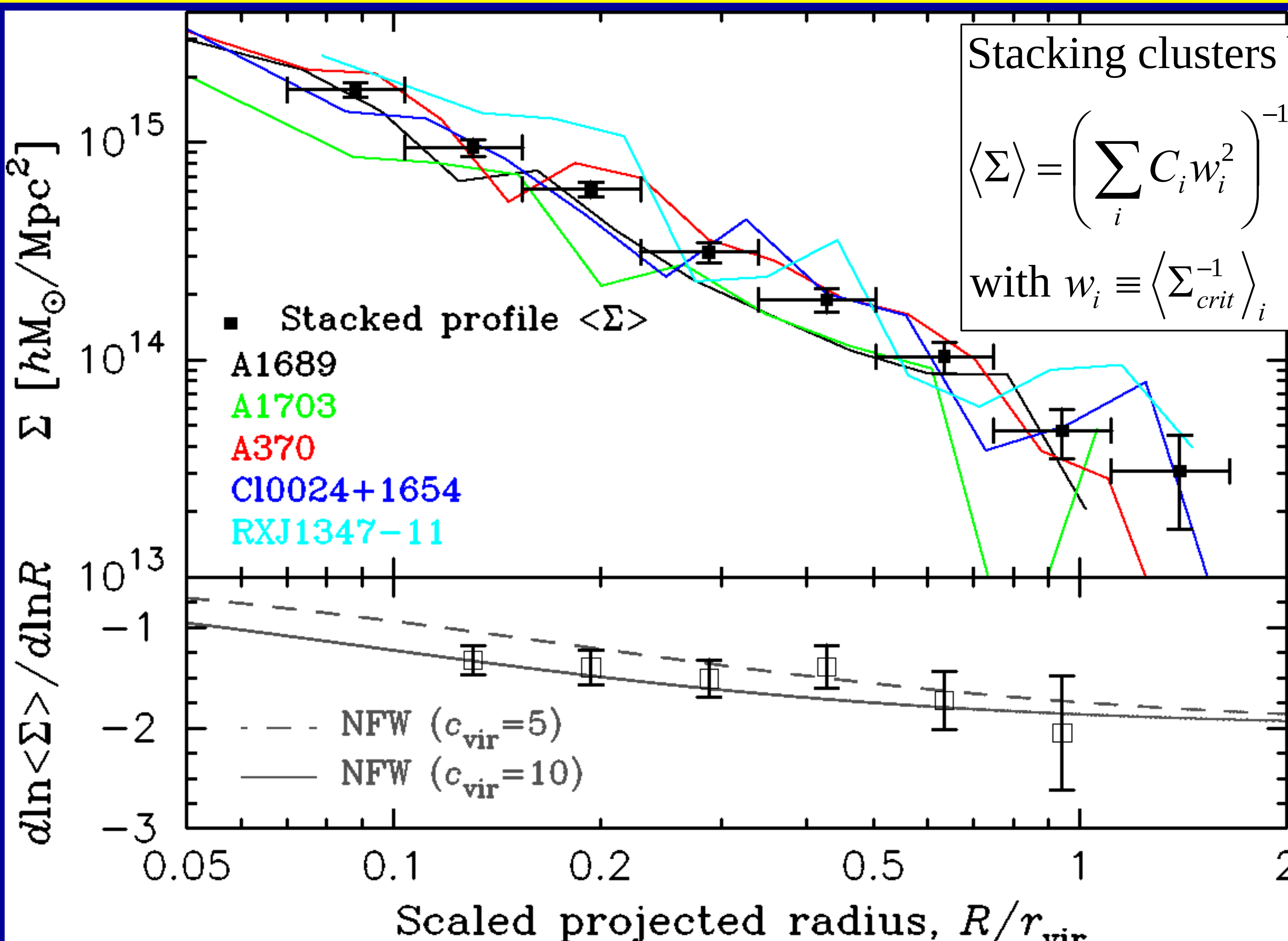

Stacking clusters by

$$\langle\Sigma\rangle = \left(\sum_i C_i w_i^2\right)^{-1}\left(\sum_i C_i w_i \kappa_i\right)$$

with $w_i \equiv \left\langle \Sigma_{crit}^{-1} \right\rangle_i$

Umetsu et al. 2010b

[2] Testing LCDM by Cluster Lensing Profiles

Compare “**WL distortion + Einstein-radius**” constraints (left) with “**WL magnification bias**” (right) in 4 high-mass clusters:

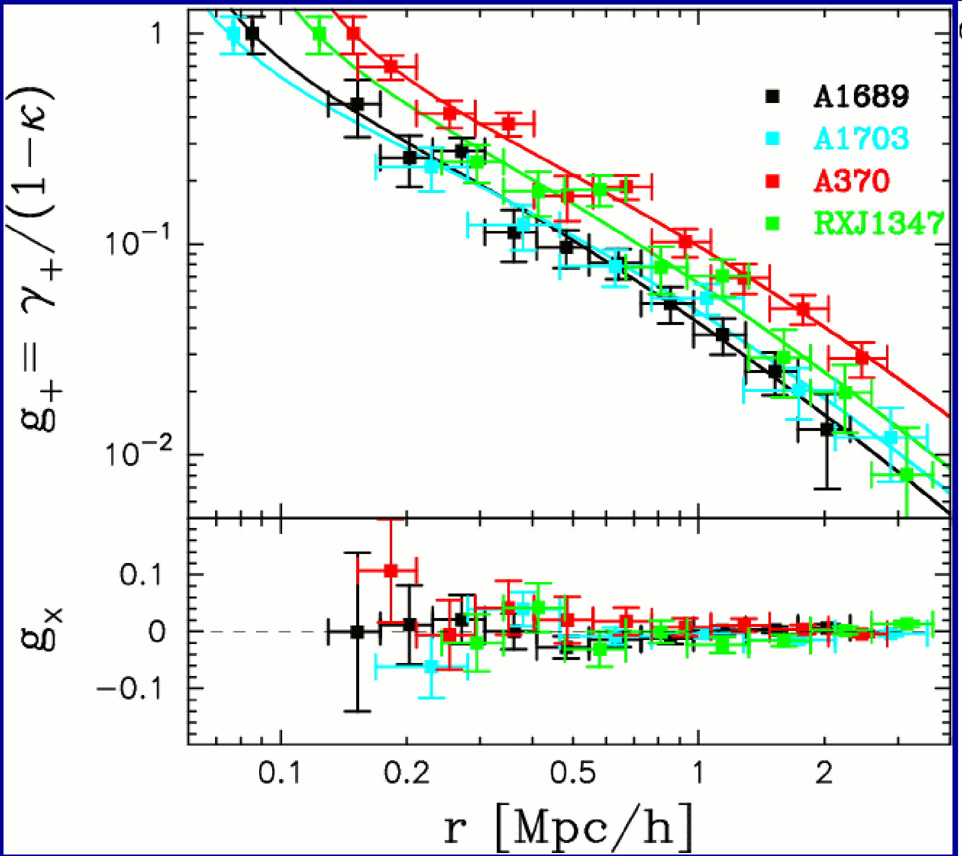

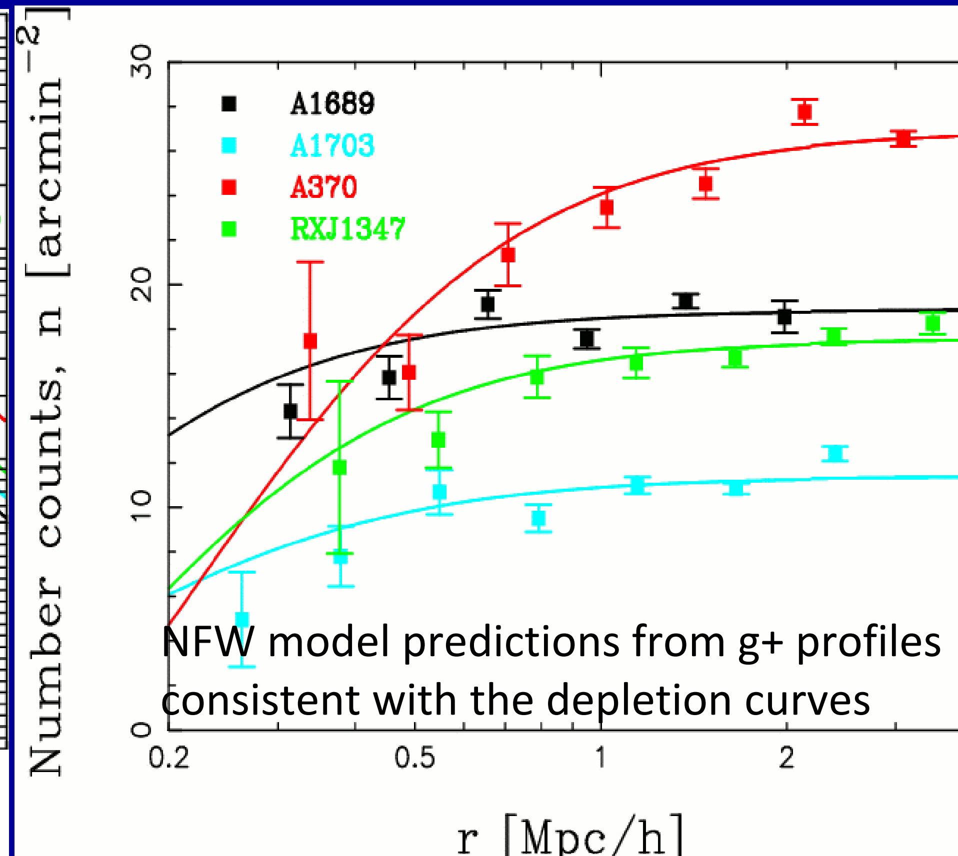

Observed curves are similar in form, well described by CDM-consistent NFW profiles

Broadhurst, Umetsu, Medezinski+ 2008, ApJ, 685, L9

First Lensing Tests of the C-M Relation

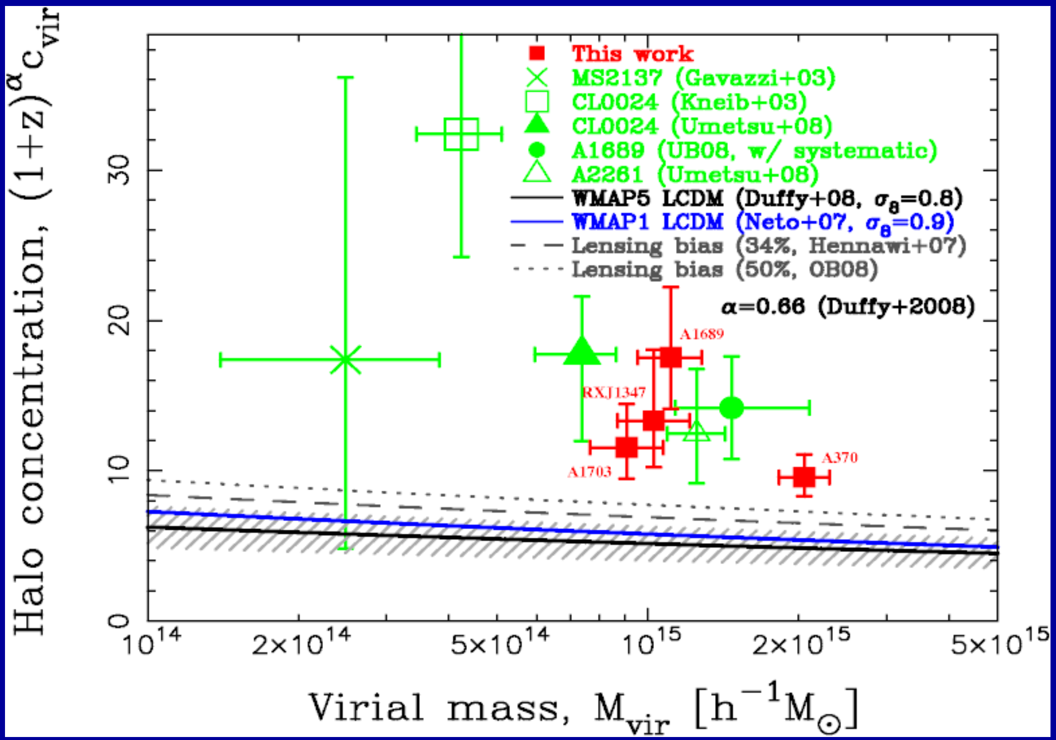

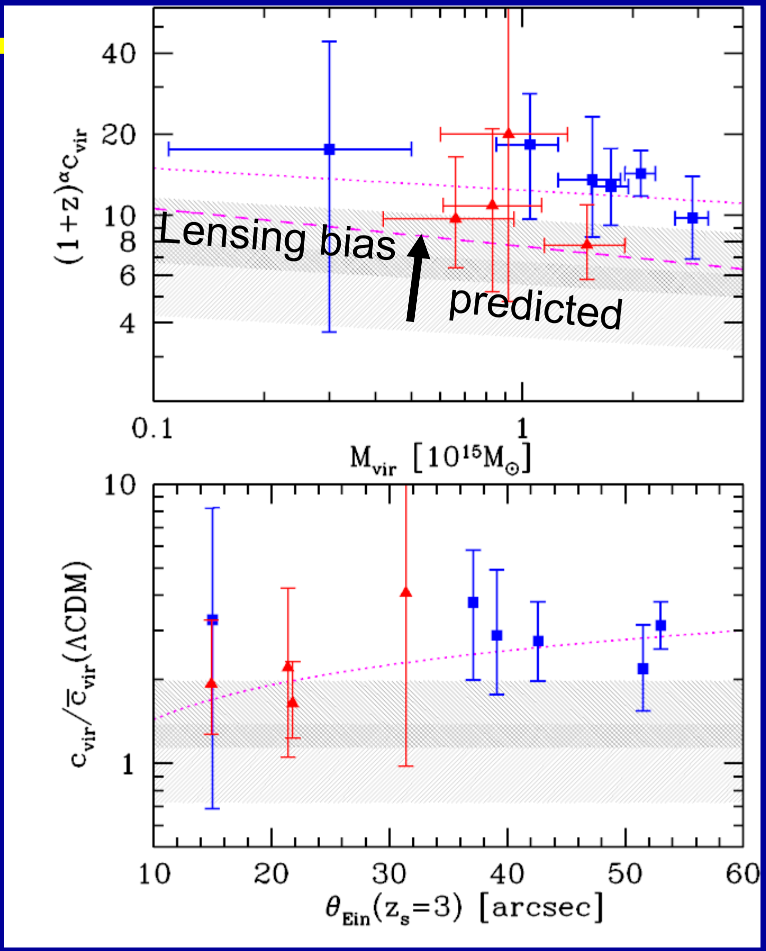

*Taking into account an orientation bias correction of +**18%,** discrepancy is still 4σ.*
*With a **50% bias** correction, it represents a 3σ deviation (BUM+2008)*

Left) Broadhurst, Umetsu, Medezinski+ 2008, ApJ, 685, L9 (BUM+2008)

Right) Oguri et al. 2009, ApJ, 699, 1038

Some (lensing-biased) clusters appear over-concentrated

The observed tendency for higher proportion of mass to lie at small radius in projection:

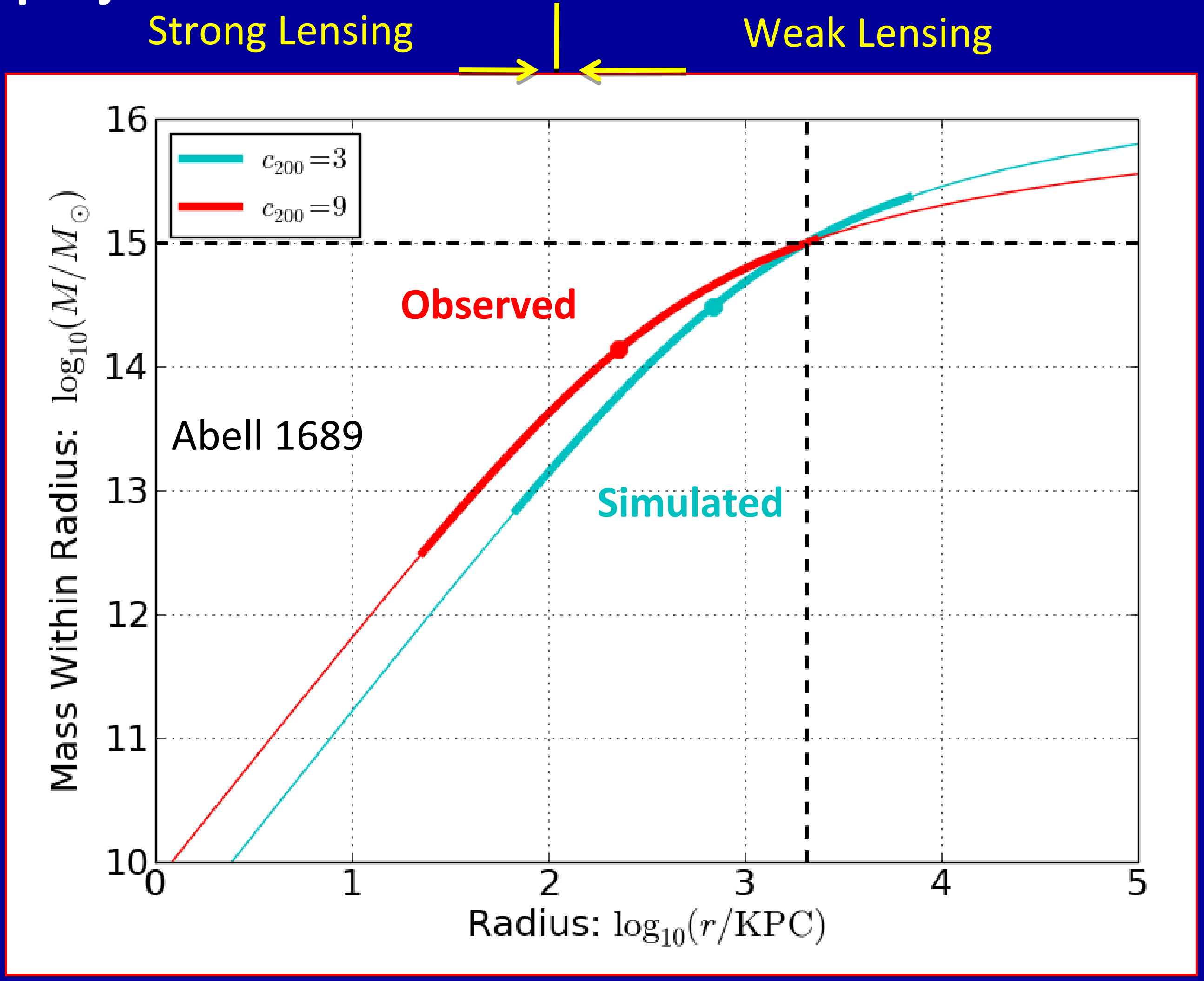

Possible explanations for high observed concentrations

- **Lensing selection bias**
  - Strong lensing bias towards intrinsically high mass concentration halos (Hennawi et al. 2007)
  - Triaxial orientation bias (Oguri & Blandford 2009)
  - Significant (25-50%) but probably not sufficient
- **Baryons and adiabatic contraction**
  - Probably not a major effect in clusters if AGN feedback is taken into account (Duffy et al. 2010; Mead et al. 2010)
  - A.C. will increase the inner cusp slope α ($\uparrow$), while shallow slopes α<~1 preferred in A1689 and CL0024+1654.
- **Clusters formed earlier than in LCDM**
  - Early Dark Energy (e.g., Sadeh & Rephaeli 2008; Grossi & Springel 2009) or primordial non-Gaussianity?

Clusters with high concentrations and early formation times *may* be giving us hints of "Early Dark Energy" (EDE)?

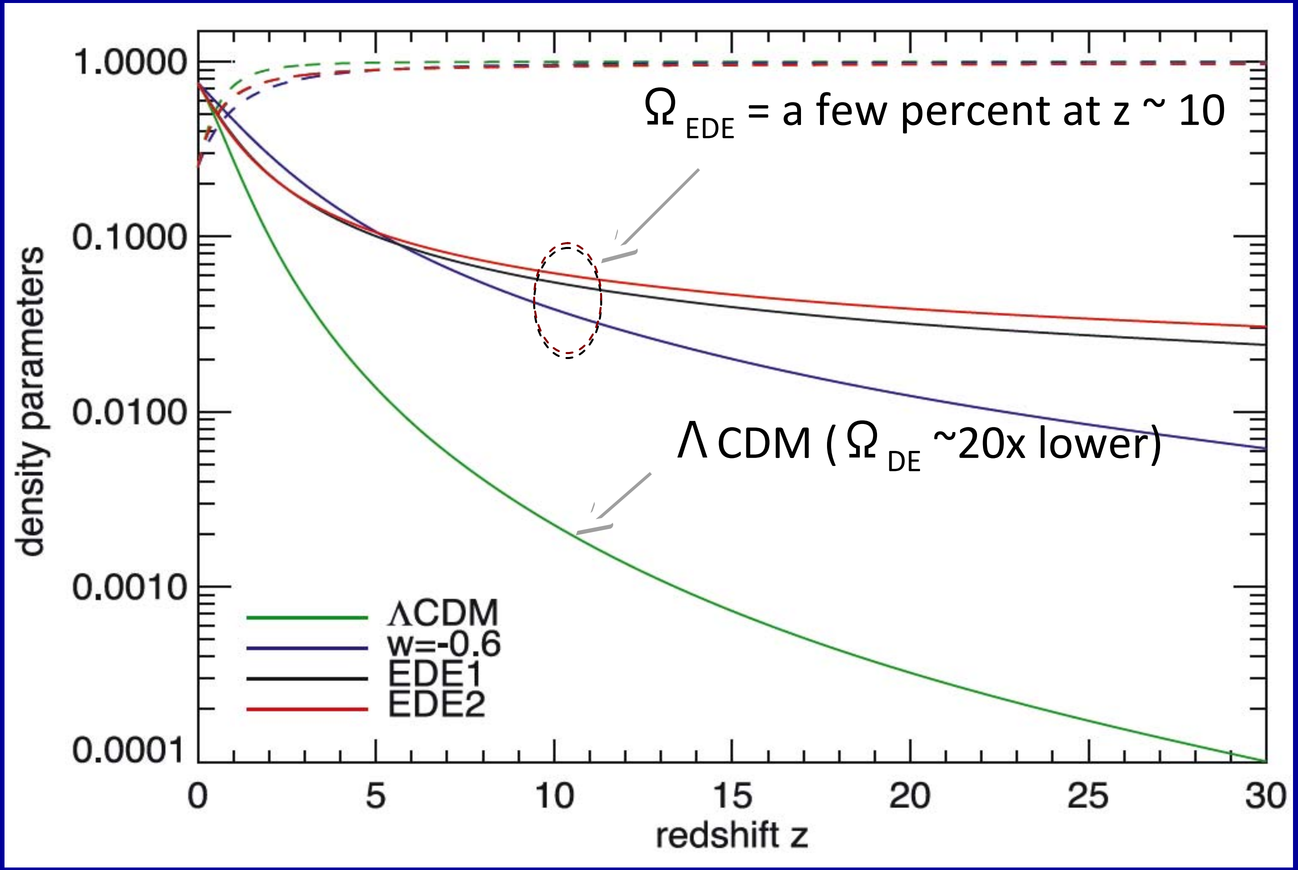

Dark energy suppresses the growth of structure.

In EDE models, cluster growth was suppressed earlier.

So clusters must have started forming earlier *to achieve the abundances observed today.*

Grossi & Springel 2009

[3] LoCuSS Stacked Cluster WL Analysis

Stacking WL distortion profiles of an "unbiased" sample of clusters

→ less sensitive to substructures/asphericity of individual clusters

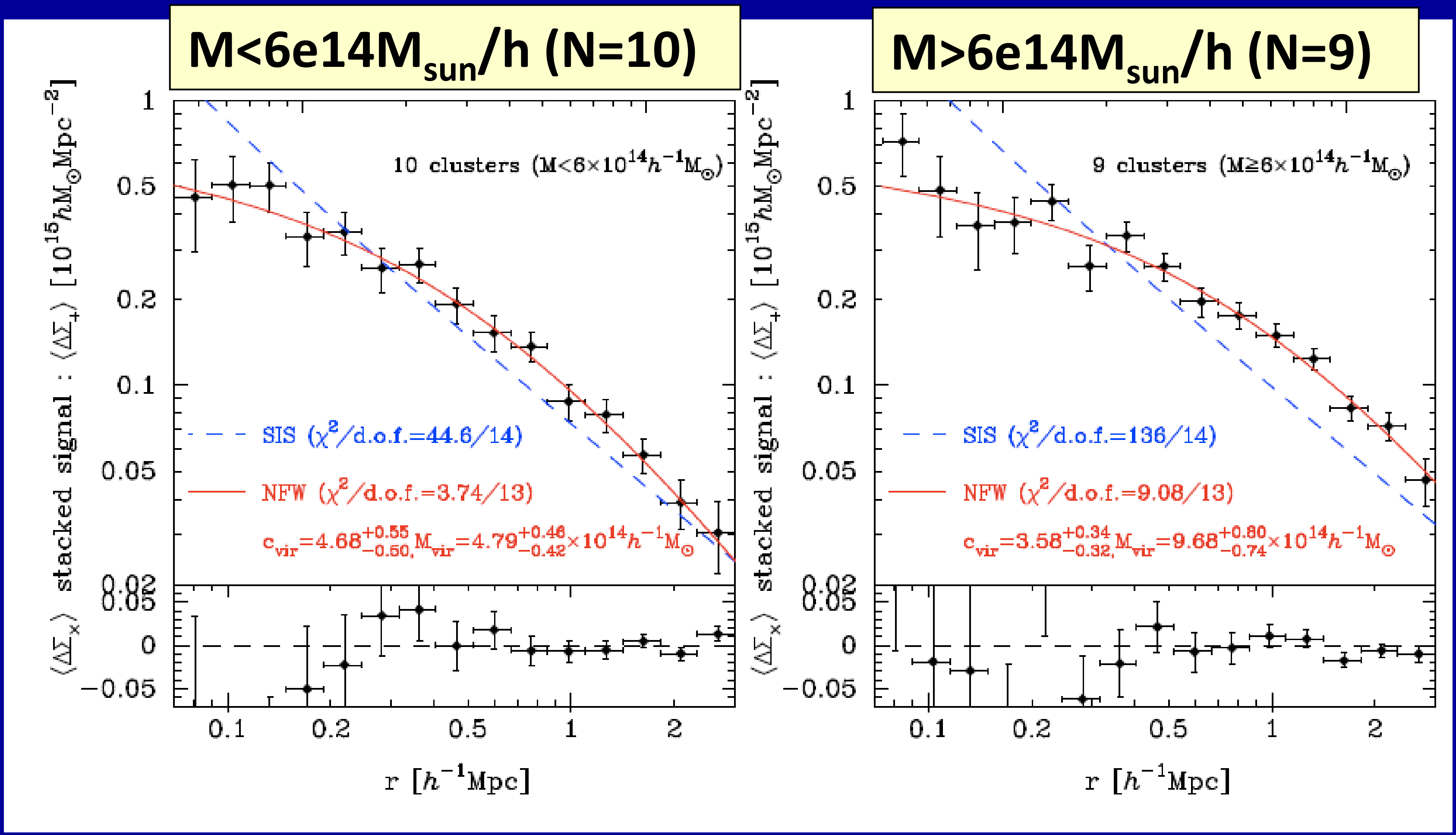

SIS rejected @6 and 11 σ levels (Okabe,Takada,Umetsu+ 10, arXiv:0903.1103)

Subaru WL Results: Observations vs. Theory

Subaru WL (19 clusters)

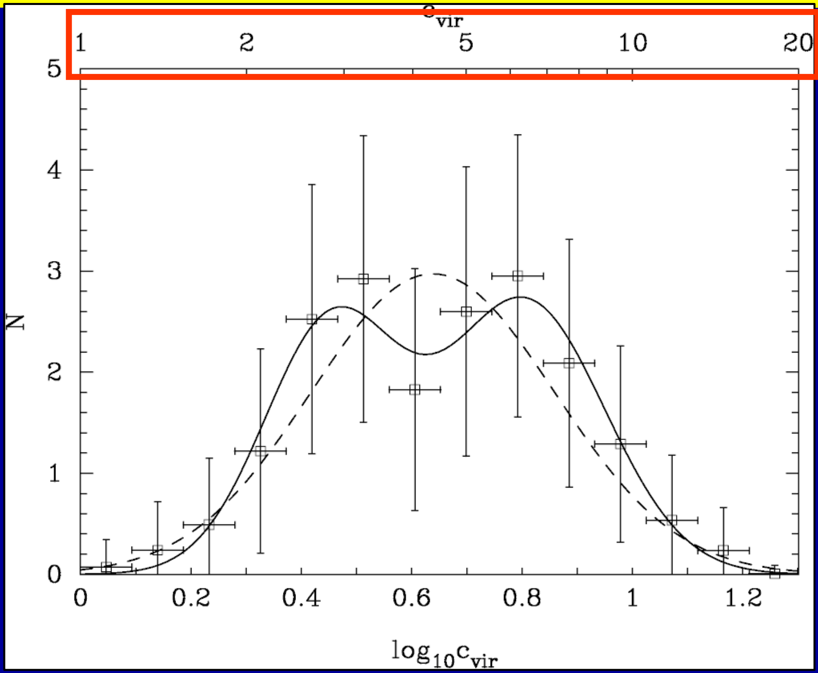

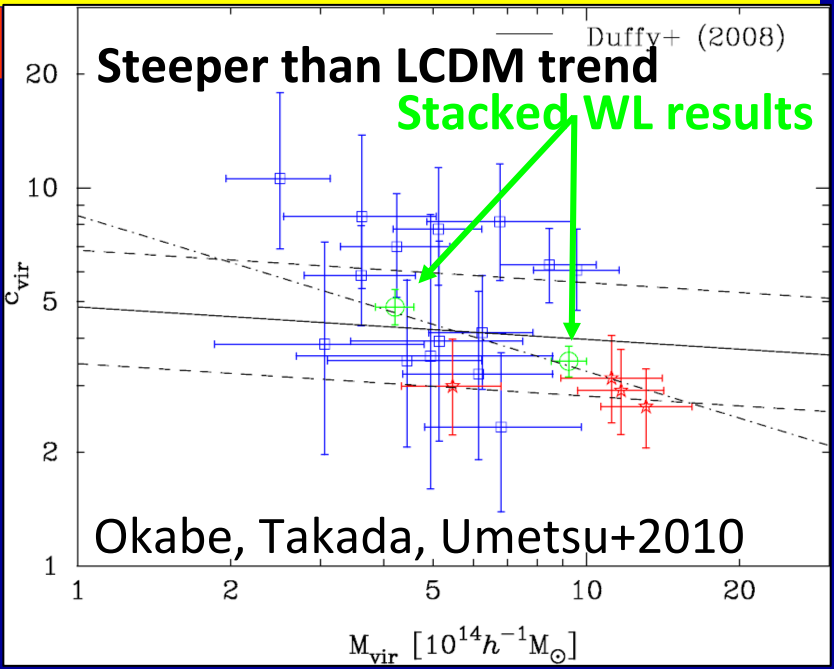

LCDM theory

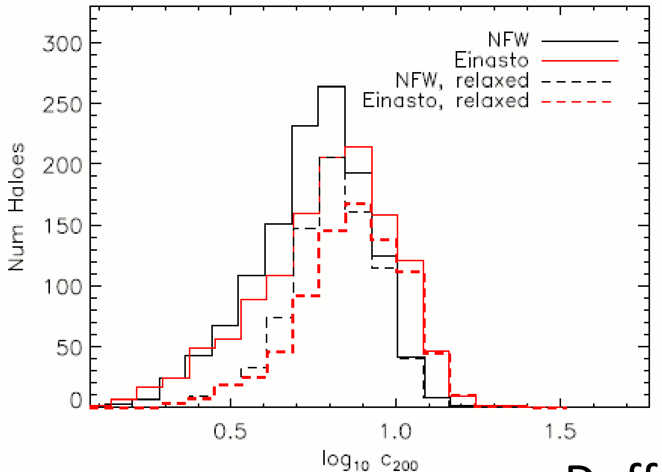

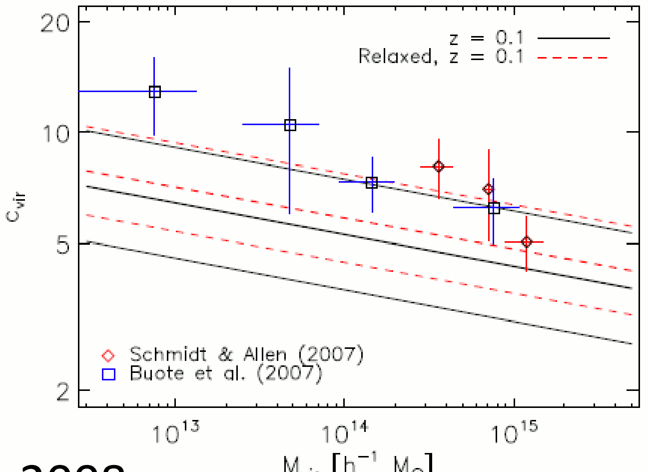

Duffy et al. 2008

[4] Weak-Lensing Distance-Redshift Relation

Medezinski, Broadhurst, Umetsu, Benitez, & Taylor 2011, MNRAS, submitted

Factorizing the distortion signal strength (in the weak lensing limit):

$$\gamma_+(\theta, z_s) \propto \frac{D_{LS}(z_s)}{D_{OS}(z_s)}\left(\bar{\Sigma}(<\theta) - \Sigma(\theta)\right) \propto \frac{r(\chi_S - \chi_L)}{r(\chi_S)}$$

$$r = r(\chi; K)$$ *Angular comoving distance*

$$\chi(z) = \int_{1/(1+z)}^{1} \frac{da}{a^2 H(a)}$$ *Comoving distance*

For a fixed cluster lens (potential and distance), the shearing signal strength $\langle\gamma_+\rangle$ is proportional to the distance ratio D_{LS}/D_{OS}.

Compare the cluster shear amplitude $\langle\gamma_+\rangle$ between two-different background populations "i,j" with different mean depths:
$\Gamma_{ij} \equiv \langle\gamma(z_i)\rangle / \langle\gamma(z_j)\rangle$ - *the shear-ratio statistic*

We expect the shear amplitude $\langle\gamma_+(z)\rangle$ increases with increasing background depth $\langle z\rangle$, purely due to the cosmological geometric effect, providing a new geometric cosmological test.

In practice, how to measure it? Is it feasible?

Background Galaxy Populations

Select **background** galaxy samples in Subaru color-color (CC) space:

- Red – background
- Blue – background
- Green – **background**
- Pink – **background** (high-z dropouts)

<z$_{phot}$> in CC-space from the 30-band photometric catalog of the 2deg^2 COSMOS survey (Ilbert et al. 2009)

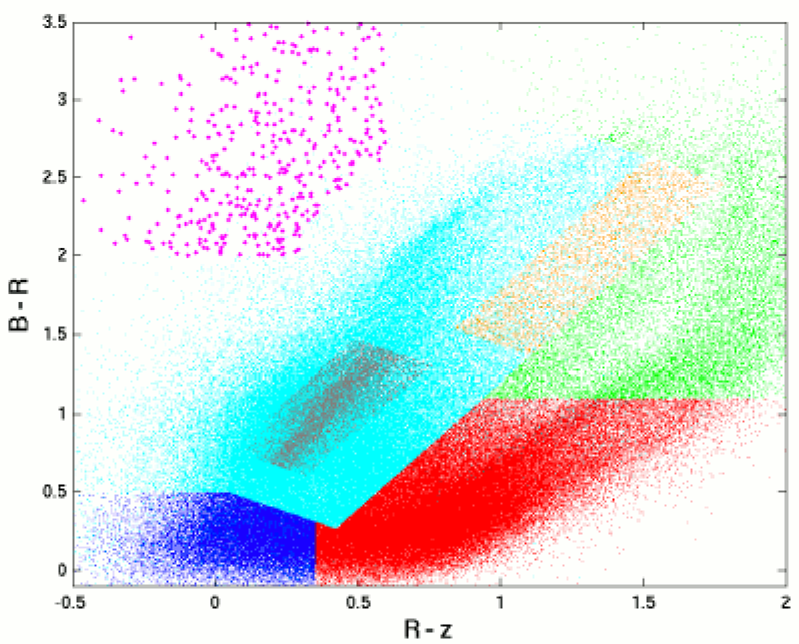

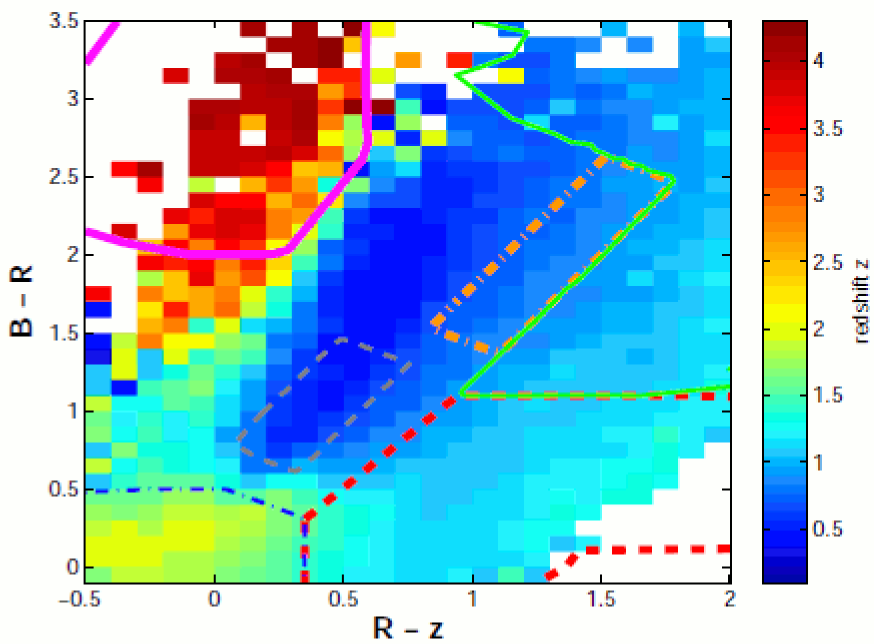

First Detection of the Shear Amplitude vs. Redshift Relation in Weak Lensing

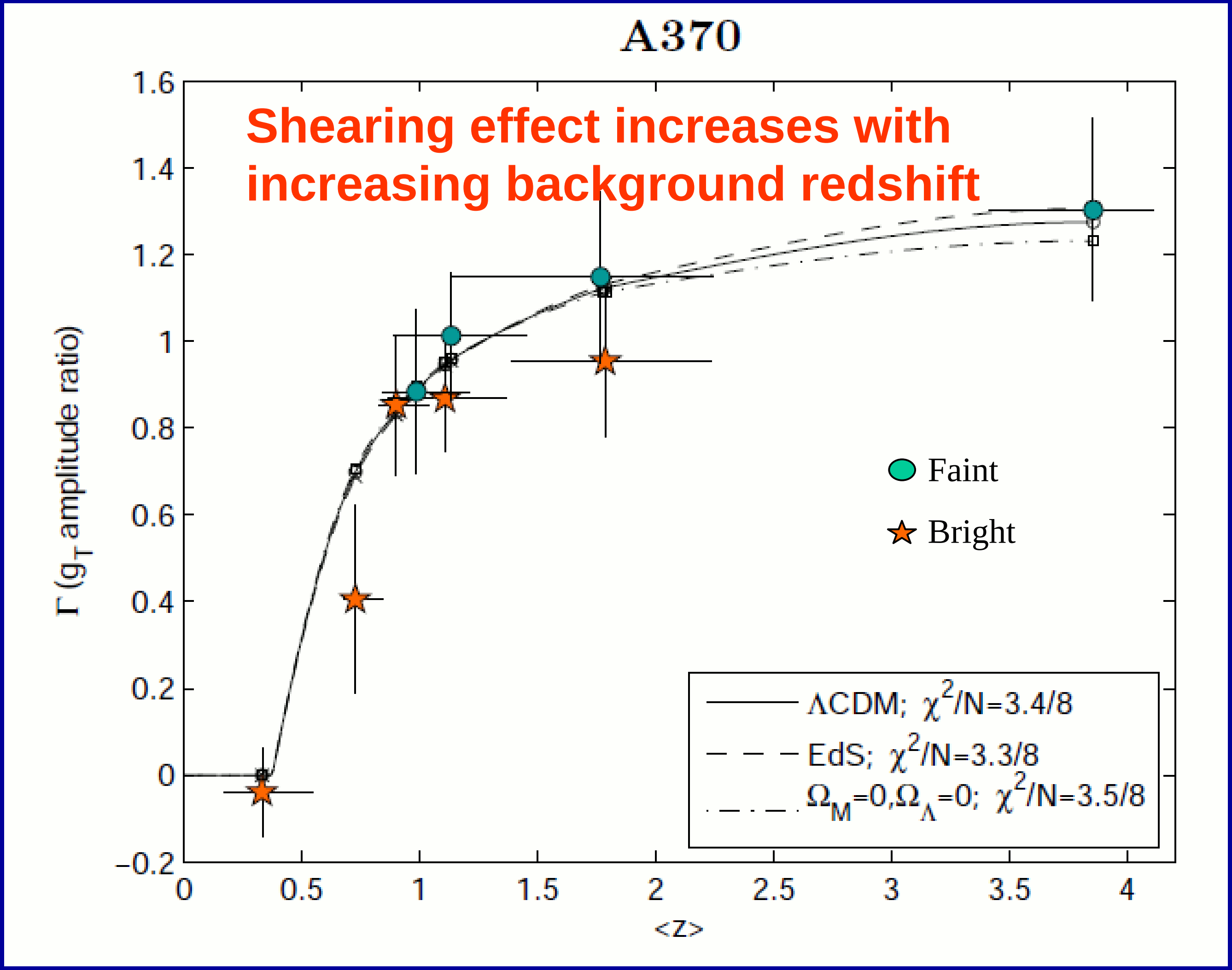

Detected in 3 massive clusters (A370, Cl0024+17, RXJ1347-11):
Medezinski, Broadhurst, Umetsu et al. 2011 (MNRAS, submitted)

Prospects for a Dark Energy Constraint

Sensitivity for the DE equation-of-state (EoS) parameter (A. Taylor et al. 2007):

$$\frac{\Delta w}{w} = \frac{2}{\gamma_t}\left(\frac{d\ln\Gamma}{d\ln w}\right)^{-1}\frac{\sigma_e}{\sqrt{N_b}},$$

Using $\Gamma(w) \sim |w|^{-0.02}$ (Taylor+ 07) and summing over background galaxies behind 25 massive clusters ($\gamma=0.05$, $\sigma_e=0.3$, $N_b=1.25\times10^6$; taking A370 as our guide), we have:

$\Delta w \sim 0.6$ @$w = -1$ (cosmological constant)

Other geometric probes (SNIa and BAO): $\Delta w \sim 0.3$

Our shear-ratio statistic has a different parameter degeneracy from others, so that combining WL with other probes will improve the sensitivity to determine the DE EoS parameter.

Summary

- **Cluster mass profile shapes**
  - Full mass profile shapes have been measured for several massive clusters from detailed strong and weak lensing analyses.
  - In all cases, the overall mass profile shows a continuously steepening radial trend, well approximated by an Navarro-Frenk-White profile expected for collisionless, non-relativistic (cold) DM.
  - Needs more clusters (~25) to definitively determine the representative mass profile shapes, in particular the inner and outer density slopes $d\ln\rho/d\ln r$, from joint WL+SL analyses.
- **Mass vs. concentration relation and its evolution**
  - High mass concentrations found for ~10 massive (strong-lensing biased) clusters from joint WL+SL analyses
  - So far cluster weak-lensing observations are focused at $0.1<z<0.3$ (e.g., LoCuSS) → needs a wide redshift coverage to higher z (~1).
- **Shear-ratio statistic as a geometric DE probe**
  - We have developed a new purely geometric method to measure the cosmological distance vs. z relation using cluster WL.
  - Currently the sample size is too small to constrain the background geometry, but the WL method is promising and can be combined with other geometric probes to better constrain DE.

CLASH:

Cluster Lensing And Supernova survey with Hubble

An HST Multi-Cycle Treasury Program designed to place new constraints on the fundamental components of the cosmos: dark matter, dark energy, and baryons.

WFC3 (UVIS + IR) and ACS will be used to image 25 relaxed clusters in 14 passbands from 0.22 - 1.6 microns. Total exposure time per cluster: 20 orbits.

Clusters chosen based on their smooth and symmetric x-ray surface brightness profiles. Minimizes lensing bias. All clusters have $T > 5$ keV with masses ranging from ~5 to ~30 x 10^{14} M . Redshift range covered: $0.18 < z < 0.90$.

Multiple epochs enable a $z > 1$ SN search in the surrounding field (where lensing magnification is low).

Marc Postman (P.I.)	Megan Donahue	Dani Maoz	Stella Seitz
Matthias Bartelmann	Rosa Gonzales-Delgado	Elinor Medezinski	Keiichi Umetsu
Narciso Benitez	Holland Ford	Leonidas Moustakas	Arjen van der Wel
Larry Bradley	Leopoldo Infante	Eniko Regoes	Wei Zheng
Tom Broadhurst	Daniel Kelson	Adam Riess	Adi Zitrin
Dan Coe	Ofer Lahav	Piero Rosati	

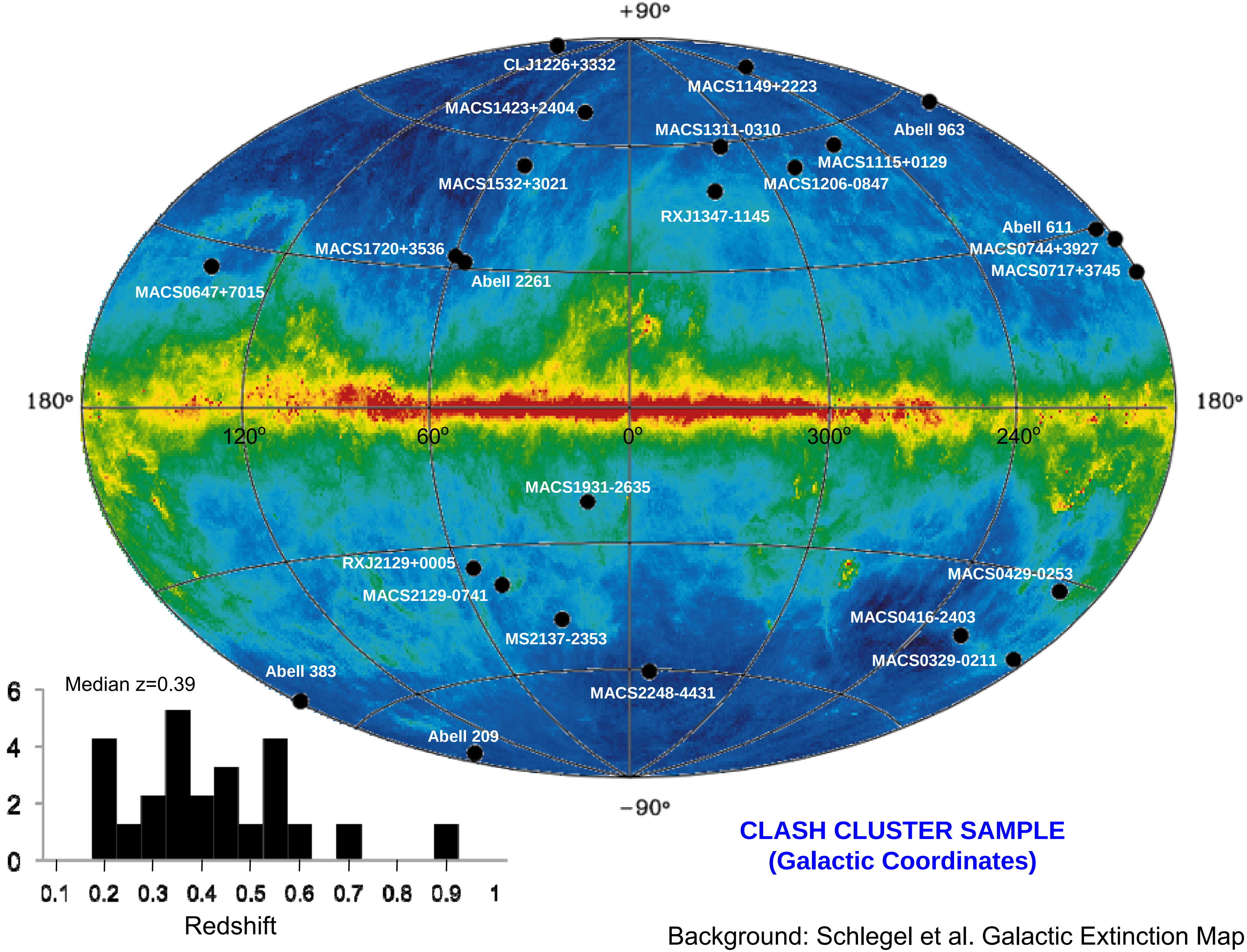
+90°
-90°
180°
180°
120°
60°
0°
300°
240°
CLJ1226+3332
MACS1149+2223
MACS1423+2404
Abell 963
MACS1311-0310
MACS1115+0129
MACS1532+3021
MACS1206-0847
RXJ1347-1145
Abell 611
MACS1720+3536
MACS0744+3927
MACS0717+3745
Abell 2261
MACS0647+7015
MACS1931-2635
RXJ2129+0005
MACS0429-0253
MACS2129-0741
MACS0416-2403
MS2137-2353
MACS0329-0211
Abell 383
MACS2248-4431
Abell 209
Median z=0.39
6
4
2
0
0.1
0.2
0.3
0.4
0.5
0.6
0.7
0.8
0.9
1
Redshift
CLASH CLUSTER SAMPLE
(Galactic Coordinates)
Background: Schlegel et al. Galactic Extinction Map

Multiple Facilities Will be Used

- HST 524 orbits: 25 clusters, each imaged in 16 passbands. (0.23 – 1.6 μm)


- Chandra x-ray Observatory archival data and possibly new data. (0.5 – 2 keV)


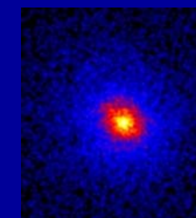

- Spitzer IR Space Telescope archival data and possibly new data (3.6, 4.5 μm)


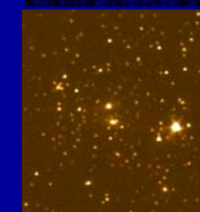

- tSZE observations proposed to augment existing data (Bolocam@150GHz, AMiBA)


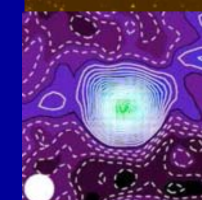

- Subaru wide-field imaging (0.4 – 0.9 μm)
- GTC, VLT, and Magellan Spectroscopy


CLASH: An HST Multi-Cycle Treasury Program

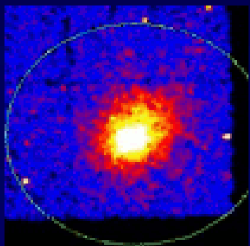
Abell 209

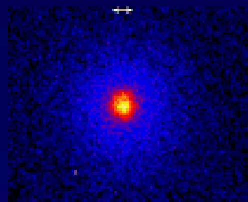
Abell 383 core

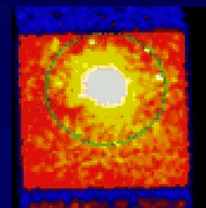
Abell 611

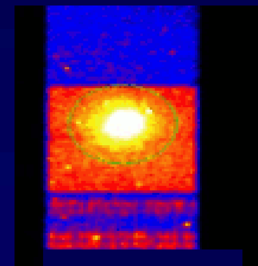
Abell 963

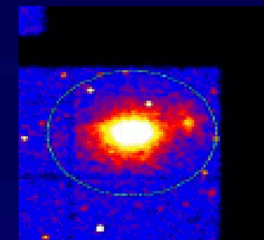
Abell 2261

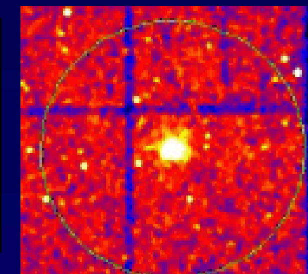
CLJ1226+3332

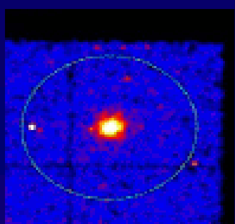
MACS 0329-0211

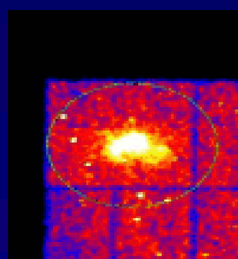
MACS 0717+3745

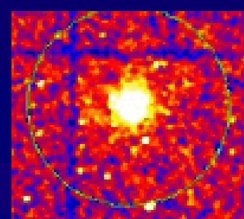
MACS 0744+3927

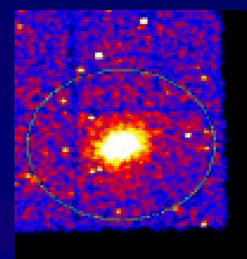
MACS 1115+0129

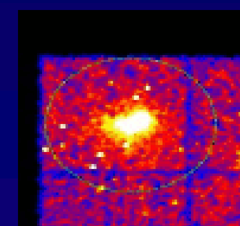
MACS 1149+2223

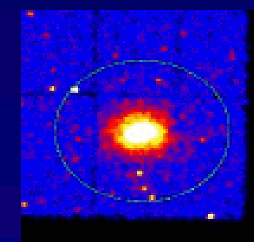
MACS 1206-0847

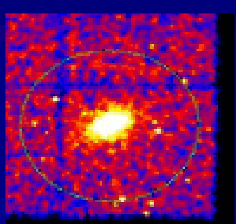
RXJ 0647+7015

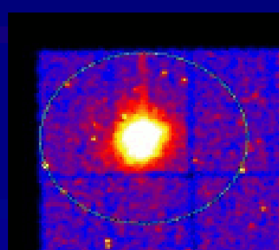
RXJ 1347-1145

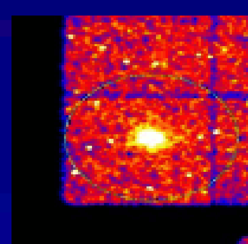
RXJ 1423+2404

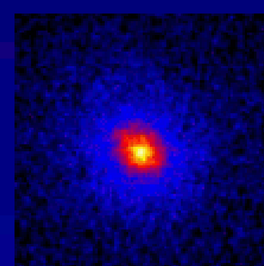
MS-2137 core

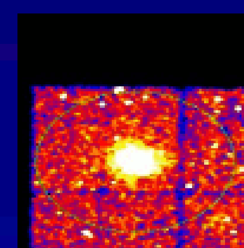
RXJ 1702+3536

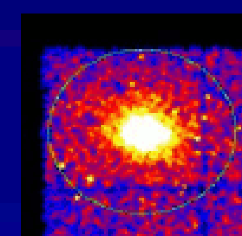
RXJ 2129+0005

Cutouts of Chandra images of 18 of the 25 CLASH clusters from ACCESS database

CLASH: An HST Multi-Cycle Treasury Program

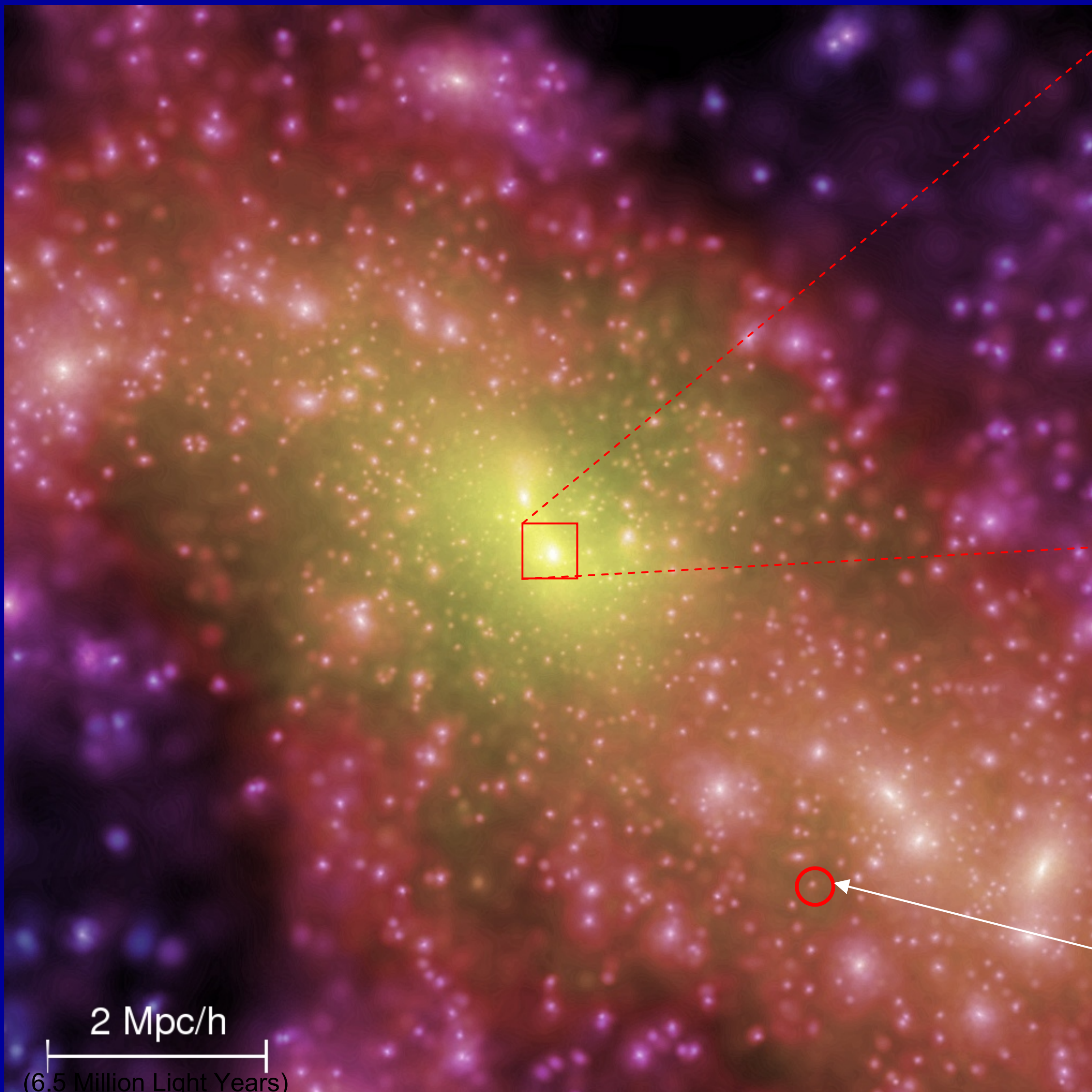

Simulation of dark matter around a forming cluster (Springel et al. 2005)

Deep HST image of massive cluster

$$R \propto \frac{\theta_{Einstein}}{\sqrt{N_{Arcs}}}$$

WHERE R IS THE RESULTING SPATIAL RESOLUTION OF THE DARK MATTER MAP

Both Strong & Weak Lensing Measurements Needed for Good Costraints

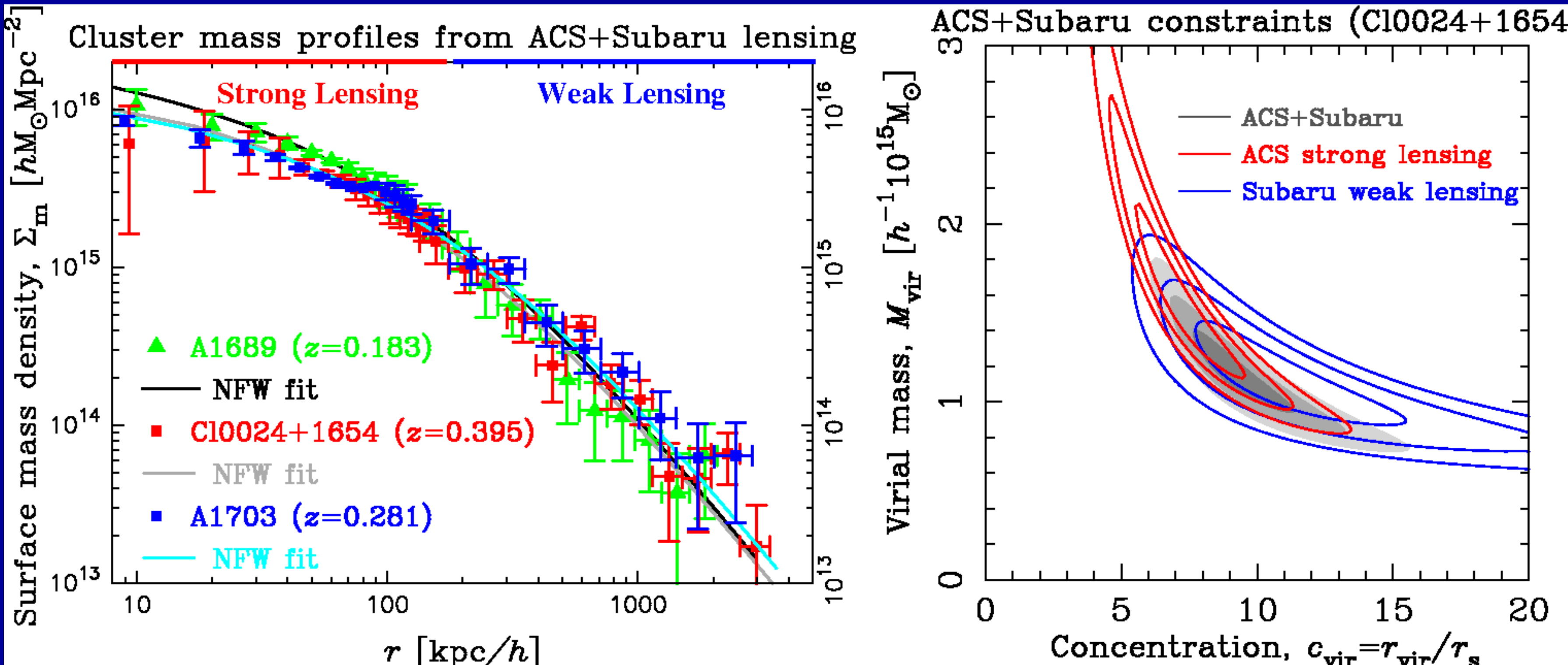

Umetsu et al. 2010

Both strong AND weak lensing measurements are needed to make accurate constraints on the DM profile.

CLASH data will allow us to definitively derive the representative equilibrium mass profile shape and robustly measure the cluster DM concentrations and their dispersion as a function of cluster mass *and their evolution with redshift.*

Nature of CDM Structure Formation

1. **Hierarchical growth**: Non-relativisitc (cold) nature of DM
   - Bottom up formation of structures in the CDM-dominated model
   - Smaller objects first form, and merge together into larger systems: i.e., galaxies -> groups -> clusters -> superclusters

2. **Anisotropic collapse**: Collisionless nature of DM
   - Gravitational collapse proceeds along sequence:
     - Collapse along smallest axis -> planar geometry ->wall
     - Collapse along middle axis -> filament
     - Collapse along longest axis -> triaxial (spheroidal) DM halos
   - Any small initial deviation from sphericity of a collapsing cloud gets magnified by tidal forces (e.g., Zel'dovich 1970; Shen et al. 2006)

After having collapsed into a clump, "virialization and emergence" of cosmic object